

2012

Factors Influencing Mercury Photoreactions in Fresh Waters: An Experimental Approach Using Light and DOC

Pin-Chin Hsu
Lehigh University

Follow this and additional works at: <http://preserve.lehigh.edu/etd>

Recommended Citation

Hsu, Pin-Chin, "Factors Influencing Mercury Photoreactions in Fresh Waters: An Experimental Approach Using Light and DOC" (2012). *Theses and Dissertations*. Paper 1193.

This Thesis is brought to you for free and open access by Lehigh Preserve. It has been accepted for inclusion in Theses and Dissertations by an authorized administrator of Lehigh Preserve. For more information, please contact preserve@lehigh.edu.

**Factors Influencing Mercury Photoreactions in Fresh Waters: An Experimental
Approach Using Light and DOC**

by

Pin-Chin Hsu

A Thesis
Presented to the Graduate and Research Committee
of Lehigh University
in Candidacy for the Degree of
Master of Science
in
Earth and Environmental Sciences

Lehigh University

April 2012

Copyright by Pin-Chin Hsu
April 2012

Thesis is accepted and approved in partial fulfillment of the requirements for the Master of Science in Earth and Environmental Sciences.

Factors Influencing Mercury Photoreactions in Fresh Waters: An Experimental Approach Using Light and DOC

Pin-Chin Hsu

Date Approved

Stephen C. Peters
Advisor

Bruce R. Hargreaves
Committee Member

Donald P. Morris
Committee Member

Frank J. Pazzaglia
Department Chairperson

Acknowledgement

I would like to express my sincere gratitude to my advisor, Steve Peters for his effort and time in instructing me, for guiding me in my research, and for correcting all the grammatical errors and awkward sentences in my thesis. He is the model of a great scientist to whom I look up to. I also want to thank my committee members, Bruce Hargreaves and Donald Morris. Bruce helped me a lot in correcting spectrophotometer and the lightmeasurement, and Don helped me a lot in the EEM. Without the expertise from all my committee members, this project could not have been accomplished.

Joe Seem, Tara Redding, Chris Dempsey, Johanna Blake, Jill Burrows, Kate Semmens, Dave Cuomo, and all EES department colleagues helped me a lot in research and lab work. Thank you for all the kind help you gave me; I really had a great time.

I want to thank the Department of Modern Language and Literature for my funding. Thank you Prof. Constance Cook, Prof. Limei Shan, and Prof. Zhansui Yu for the support in my teaching.

I want to thank my advisors in Taiwan: Prof. Shian-Chee Wu, Prof. I-Wen Su, and Prof. Che-Chen Chang, for their encouragement and help, which enabled me to pursue my dream of studying in the United States.

Thanks to my parents, Jin-Tu and Bi-Fang, who supported and believed in my dream of studying abroad.

I especially thank Vanessa Wang for her great help and understanding. She is usually the first to read my writing and listen to my rehearsals. I am really grateful for her patience and support during these two years.

Table of Contents

| | |
|--|----------|
| List of Tables | Page vi |
| List of Figures | Page vii |
| Abstract | Page 1 |
| Chapter 1: Introduction to the factors influencing mercury photoreactions in fresh waters | Page 2 |
| Chapter 2: The wavelength dependence of coupled DOC-mercury photoreduction | Page 5 |
| Chapter 3. Supporting information | Page 53 |
| Curriculum Vitae | Page 71 |

List of Tables

| | |
|--|---------|
| Table 1. DGM production and percentage of total mercury | Page 23 |
| Table 2. Comparison of cumulative DGM production, DGM production rate and photoefficiency | Page 31 |
| Table 3. Major fluorescent peaks of aquatic DOC in the EEMs | Page 44 |
| Table 4. Photoefficiency model apply to the situation under the same situations with Peters et al. 2007 research | Page 50 |
| Table 5. DGM production for all experiments | Page 55 |
| Table 6. Photoefficiency for all experiments | Page 56 |
| Table 7. DGM production under different DOC and mercury concentration | Page 57 |
| Table 8. Excitation Emission Matrices (EEMs) peak values | Page 59 |
| Table 9. Fit curves used for photoefficiency | Page 60 |

List of Figures

| | |
|--|---------|
| Figure 1. Mercury formation and transport cycles | Page 3 |
| Figure 2. Mercury and DOC reaction in the water columns | Page 7 |
| Figure 3. Possible mercury emission mechanism under different light characteristics | Page 8 |
| Figure 4. Experimental apparatus for light exposure using optical bandpass filter | Page 12 |
| Figure 5. Tekran 2500 Cold vapour atomic fluorescence spectroscopy (CVAFS) with Mercury injection system and Labview controlling program | Page 14 |
| Figure 6. Cumulative DGM production over 8 hours light exposure using different optical bandpass filter with Suwannee River NOM and Hg | Page 19 |
| Figure 7. Suwannee River DOC solution' transmitted light irradiance and absorbed Light intensities | Page 21 |
| Figure 8. Cumulative DGM production over 8 hours light exposure using different optical bandpass filter with Nordic Reservoir NOM and Hg | Page 24 |
| Figure 9. Nordic Reservoir DOC solution' transmitted light irradiance and absorbed Light intensities | Page 25 |
| Figure 10. The average photoefficiency under different filters with Suwannee River DOC solutions and Nordic Reservoir DOC solutions | Page 27 |
| Figure 11. The Excitation Emission Matrices (EEMs) before and after adding mercury for Suwannee River and Nordic Reservoir DOC solution | Page 28 |
| Figure 12. The Excitation Emission Matrices (EEMs) for Suwannee River DOC solution before and after light exposure | Page 29 |
| Figure 13. The Excitation Emission Matrices (EEMs) for Nordic Reservoir | |

| | |
|---|---------|
| DOC solution before and after light exposure | Page 30 |
| Figure 14. DGM production increase ratio with the increase of light intensity | Page 34 |
| Figure 15. DGM production rate for all data sets | Page 36 |
| Figure 16. Photoefficiency for all data sets | Page 38 |
| Figure 17. Absorbance change for two DOC solutions | Page 40 |
| Figure 18. Absorbance change for Suwannee River and Nordic Reservoir DOC solutions | Page 42 |
| Figure 19. Suwannee River NOM solution EEM compared with Suwannee River Humic Acid (SRHA) and Suwannee River Fulvic Acid (SRFA) | Page 45 |
| Figure 20. Nordic Reservoir NOM solution EEM compared with Nordic Reservoir Humic Acid reference (NAHAR) and Nordic Reservoir Fulvic Acid reference (NAFAR) | Page 46 |
| Figure 21. Photoefficiency fit curve and predicting DGM production | Page 49 |
| Figure 22. Light source spectrum for UVB, UVA , and visible light | Page 54 |
| Figure 23. Reconstructed solar irradiance for Lake Gile | Page 61 |
| Figure 24. Photoefficiency under different mercury concentration | Page 62 |
| Figure 25. Absorbance change at specific wavelength for Suwannee River DOC solutions after 105 hours light exposure using UVA with/without filter | Page 64 |
| Figure 26. Absorbance change at specific wavelength for Suwannee River DOC solutions after 105 hours light exposure using UVB with/without filter | Page 65 |

Abstract

Mercury is a toxic chemical that can harm human health through exposure. In aquatic systems, dissolved Hg^{2+} can be chemically reduced to elementary mercury Hg^0 (DGM), which volatilizes across the water/air interface into the atmosphere. The emission rate of Hg from water is the net result of mercury reduction and oxidation reactions followed by diffusion of the DGM to the surface. Mercury reduction and oxidation reactions are controlled by two factors: 1) the quality and quantity of incoming light and 2) the photo-reactivity of dissolved organic carbon (DOC). This study uses optical bandpass filters to select narrow wavebands of light to determine the wavelength dependence of DGM production. The results show that the photoefficiency (DGM per unit of absorbed light intensity) increases with decreasing wavelength of light. Two DOC sources (Suwannee River NOM and Nordic Reservoir NOM) were used to characterize the effect that DOC type would have on the emission reaction. Both DOC source and concentration influence DGM production, with the Nordic Reservoir producing more mercury. Using excitation emission matrices (EEMs) helps identify the different fluorescent moieties between the two DOC types. A model combining the photoefficiency curves with solar information was used to predict DGM emissions in the natural environment. These predictions compare favorably with existing measured emission values.

Chapter 1: Introduction to the factors influencing mercury

photoreactions in fresh waters

Mercury is a toxic chemical that can harm human health through exposure. At 25°C and 1 atm pressure, mercury exists in different physical states and chemical forms and readily moves between the atmosphere, water, soil, sediment and living organisms. Different forms of mercury have different toxicity levels. The most toxic form is methylmercury (CH₃Hg), which exists in natural ecosystems. Severe human diseases were reported in wide-ranged places around the world and considerable research has been conducted to investigate the methylmercury problem in fish. Elemental mercury (Hg⁰) can be found in thermometers or in coal-burning power plants. Because elemental mercury can travel in the vapor phase through the atmospheric circulation for up to a few years, it affects areas up to thousands of miles away from sources of emission. Inorganic mercury salts exist in nature in the forms like mercuric sulphide (HgS) and mercuric oxide (HgO). Inorganic mercury would dissolve into water, soil, and sediments and affect aquatic system (USEPA, 1997). Characterizing where and how potentially dangerous mercury travels enables scientists to more effectively manage mercury in the environment.

When studying the mercury cycle, it is helpful to understand how the varying chemical forms and the influencing factors control transportation and transformation mechanisms. This research focuses on aquatic systems, especially freshwater systems. In aquatic systems, mercury exists in ionic forms, primarily as oxidized Hg²⁺ complexes and has two main transporting paths. When Hg²⁺ is chemically reduced to elementary

mercury Hg^0 in water column, it forms dissolved gaseous mercury (DGM). The relatively insoluble DGM volatilizes across the water/air interface into the atmosphere. When bacteria methylate ionic mercury Hg^{2+} to methylmercury $[\text{CH}_3\text{Hg}]^+$, the methylmercury can be absorbed by living organisms. Since methylmercury can biomagnify up the food web in living organisms, it can affect the whole ecosystem (Clarkson, 2002).

The process of mercury emission from water to the atmosphere is the main focus of this research. The emission rate of Hg from water is governed by the production of DGM, which is the net result of mercury reduction and oxidation reactions (Figure 1). Mercury reduction and oxidation reactions are highly influenced by light, although the precise nature of how intensity and wavelength influence this reaction is still unclear.

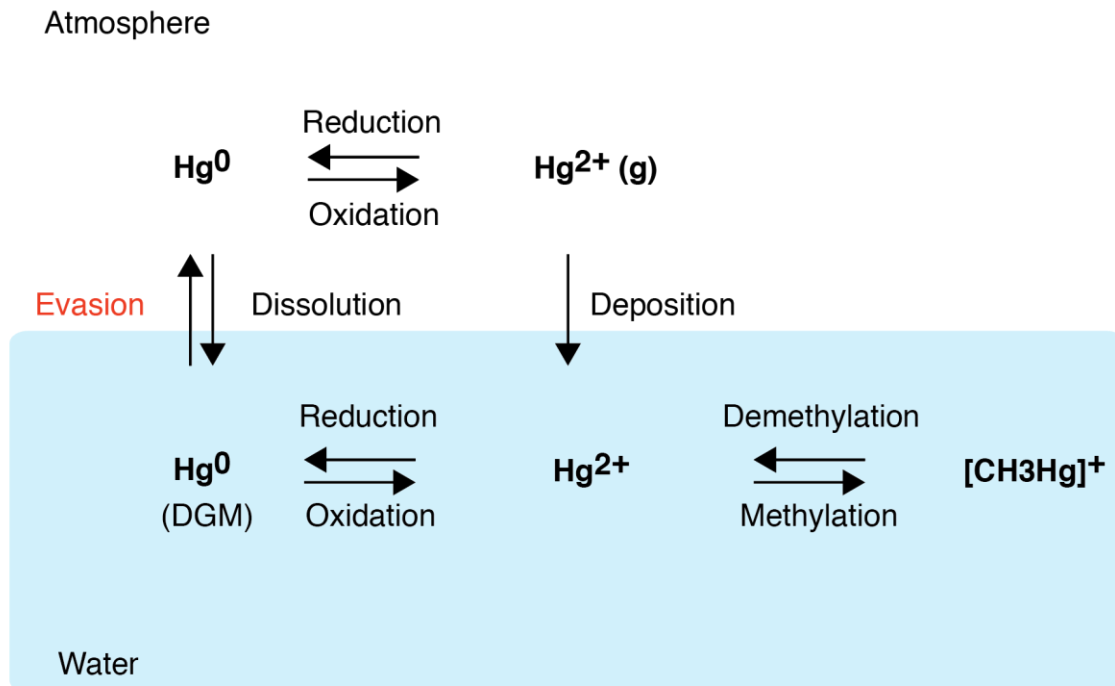


Figure 1. Mercury formation and transport cycles.

Mercury reduction and oxidation reaction are mostly control by two factors: 1) the quality and quantity of incoming light and 2) dissolved organic carbon (DOC). This study used optical bandpass filters to select narrow wavebands of light to determine the wavelength dependence of DGM production. The results showed photoefficiency (DGM per unit of absorbed light intensity) increases with decreasing wavelength of light. Two DOC sources (Suwannee River Natural Organic Material and Nordic Reservoir Natural Organic Material) were used to characterize the effect that DOC type would have on the emission reaction. The result provides a foundation to later analyze the mercury emission at different water columns around the world. By investigating mercury reduction in a freshwater system, we not only can understand better the global mercury cycle but also can more precisely estimate the amount of mercury available for methylation to methylmercury.

Chapter 2: The wavelength dependence of coupled DOC-mercury photoreduction

1. Background and Introduction

Mercury flux from aquatic systems has long been regarded as an important issue since it greatly influences the global mercury cycle. When mercury emits from the aqueous to atmospheric environments, it can move long distances from its original pollution source. When mercury methylates into methylmercury, it accumulates in the food chain and can severely damage human health. Understanding the fate and transport of mercury can provide a better idea of how to avoid potential environmental exposure.

Most previous research has been focused on how methylmercury bioaccumulates in the food web and influences the ecosystem. Fewer studies investigate the mercury transition from water into the atmosphere, which is crucial to knowing how much mercury remains behind in the aquatic system and is available for methylation. Since methylmercury has the highest toxic effect out of all mercury forms and impairs human health the greatest, there is a crucial need to understand the factors that control mercury emission rates.

Mercury emission from water into the atmosphere is believed to be highly influenced by three main factors: 1) light intensity and wavelength, 2) the quality and quantity of dissolved organic carbon (DOC), and 3) the abundance of mercury bound to DOC and not complexed with other ligands (Vost et al., 2012). Light appears to dominate the mercury emission mechanism. For example, the dissolved gaseous mercury (DGM) emission in several lakes was lowest during nighttime and highest around noon

(Amyot et al., 1994, Krabbenhoft et al., 1998). Since then, scientists have been trying to understand how mercury emission relates to specific properties of light. DGM formation was found to be influenced by light intensity and other factors in temperate and arctic lakes. (Amyot et al., 1997a and 1997b).

The emission of DGM is proportional primarily to light intensity along with other factors in temperate and arctic lakes. (Amyot et al., 1997a and 1997b). Decreasing light penetration into water decreases DGM production rates, confirming the importance of light intensity (Wollenberg and Peters, 2009).

In aquatic environments, mercury is usually bound to dissolved organic carbon (DOC, Figure 2). Among all the functional groups, mercury would bind to thiol or sulfur-containing groups more easily (Xia et al., 1999, Hesterberg et al., 2001, Ravichandran 2004, and Skyllborg et al., 2006). DOC also contains numerous chromophores that interact with photons. When light penetrates into water, light would interact with the chromophore, and can break bonds to “photobleach” the DOC. The photobleaching reaction liberates some electrons, which can be donated to mercury and the mercury is thus reduced from Hg^{2+} to Hg^0 . Since Hg^0 (DGM) does not bind to DOC nor is it soluble in water, it would escape into the atmosphere very quickly.

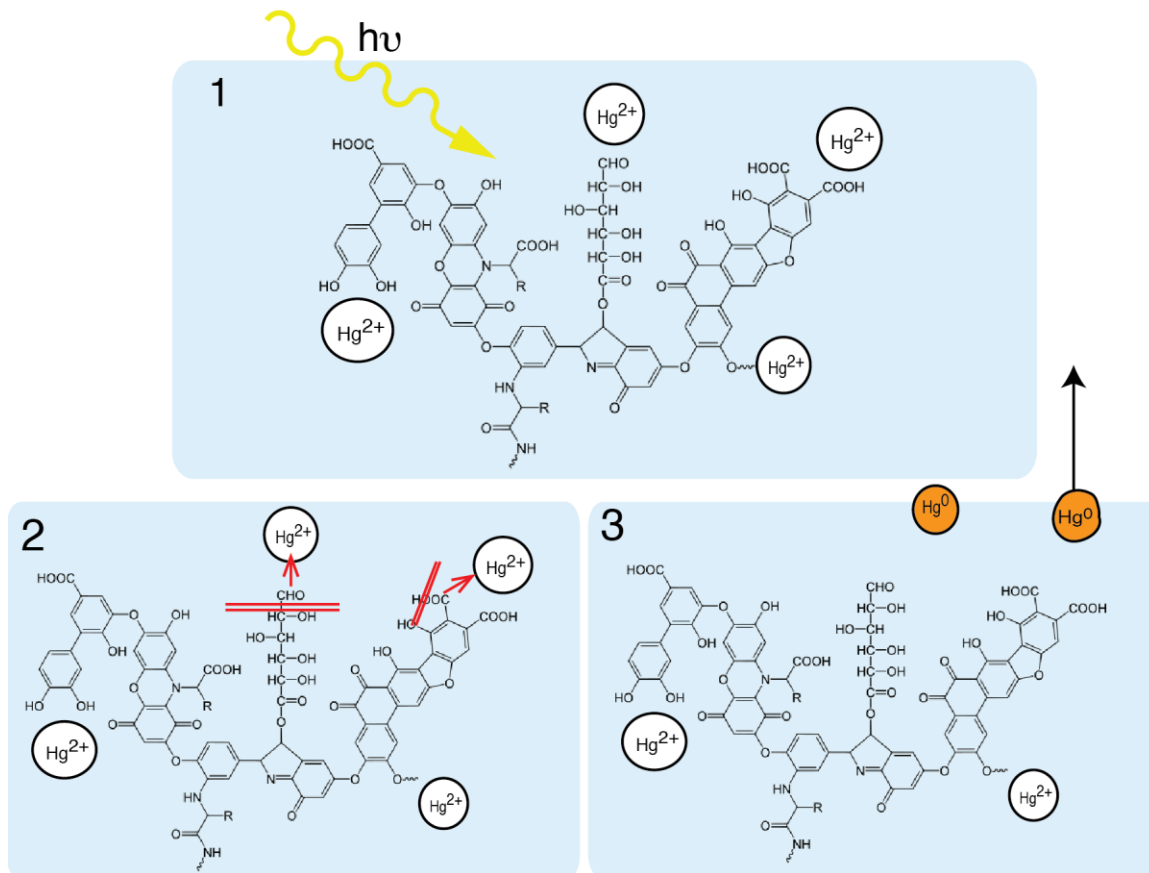


Figure 2. Mercury and DOC reaction in the water columns. The DOC listed here is humic acid.

Despite our current understanding of how light interacts with DOC and mercury, one item remains unclear - How does light affect mercury emission? Natural sunlight consists of mostly visible light (400 – 700 nm) and only a small portion of ultraviolet radiation (UV). UV light consists of more than 95% UVA (320 – 400 nm), and the remaining UVB (280- 320 nm). However, the most effective photobleaching wavelengths are in the UV bands (Kirk 1994). There are three possible determining factors for how incident light might affect mercury emission: light quantity (abundance), light quality (energy per photon), or specific wavelength (Figure 3). Overall light quantity is positively correlated with DGM production (Amyot et al. 1997a and 1997b). However, shorter

wavelengths of light may be more important at lower intensity while we can't rule out the possibility of most effective DGM production at specific wavelengths.

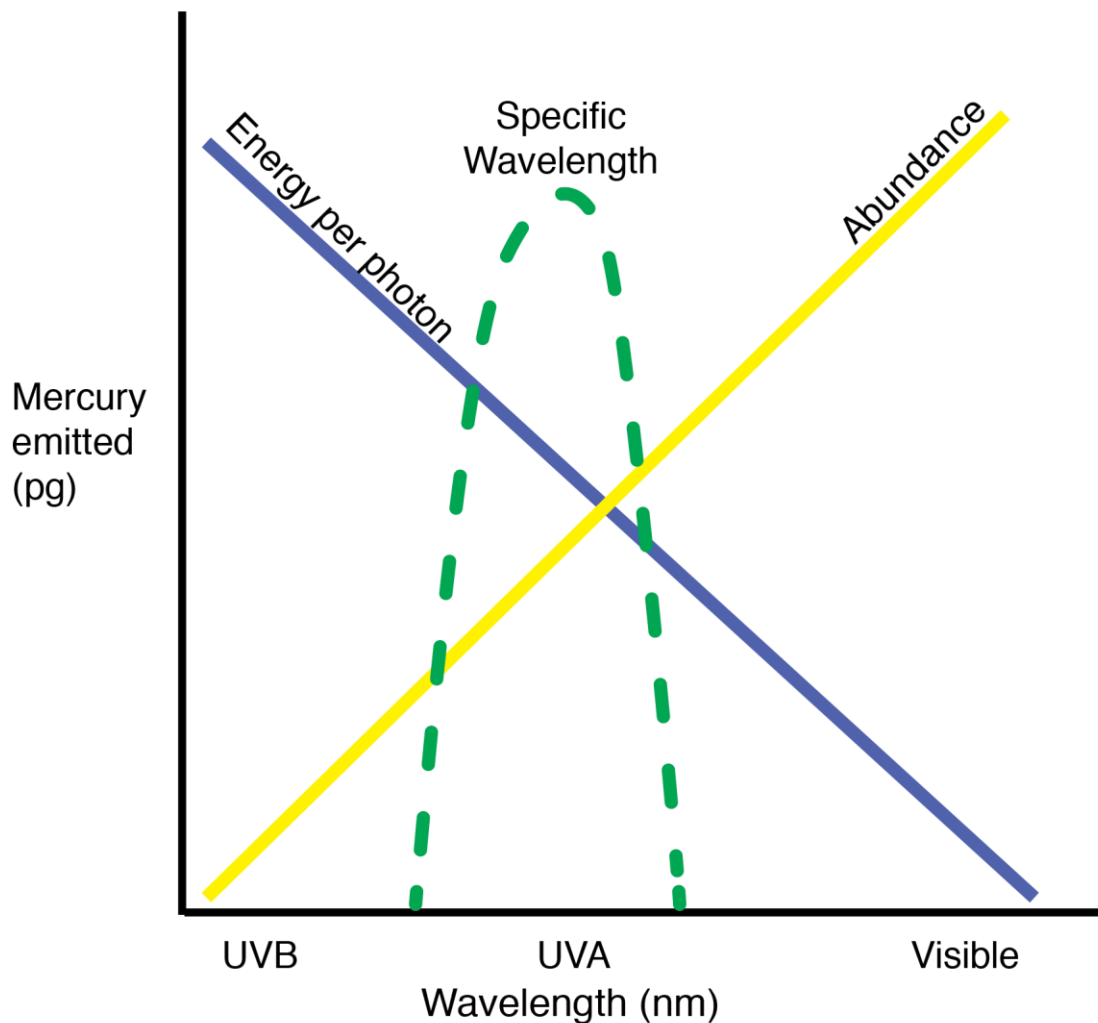


Figure 3. Possible mercury emission mechanism under different light characteristics. Natural sunlight contains mostly visible light, but UV lights have stronger energy per photon. Specific wavelength might also be crucial for the mercury duction reaction.

Visible light accounts for the highest portion of natural sunlight. However, by the Planck–Einstein equation, the light intensity can be calculated by $E = hc/\lambda$, where h is the Planck constant, c is the speed of light and λ is the light wavelength. From the equation, ultraviolet light with shorter wavelength would have higher energy per photon than

longer wavelengths of light. Some researchers claim that UV light is more important in mercury reduction in aquatic system, however, opinions differ on whether it's UVA or UVB that's the key. The majority of researchers argue that UVB is the most effective driver for mercury photoreduction (Oh et al. 2011, Qureshi et al. 2010, O'Driscoll et al. 2006), while some said it is UVA under high DOC concentration (Garcia and Amyot, 2005, Amyot et al. 1994). Nevertheless, all these studies share a common flaw: that is, the light source they used- the UV lamp- had a broad band spectrum, meaning the UVB source contained UVA while UVA source also contained UVB. The overlapping light makes the conclusions questionable. A more accurate and precise way of examining the influence of light is needed to fully explain the mercury emission mechanism.

In this study, I utilize optical bandpass filters to select a specific wavelength of light to expose lab-incubated solutions, and I also measure each solution's light irradiance with a calibrated spectroradiometer. The spectral absorbance of the experiment solution is also measured to calculate absorbed energy. By directly studying the relationship between certain wavelengths of light and mercury photoreduction along with the solution absorbed energy, this study may be able to answer a long-standing problem in mercury photoreaction kinetics. Two DOC sources (Suwannee River NOM and Nordic Reservoir NOM) were also used to characterize the effect that DOC type would have on the mercury emission. By realizing the main factors controlling mercury emission in water systems, we could better understand the global mercury cycle and reduce the risk for possible mercury exposure.

2. Method

2.1 Light sources

Sunlight contains a broad spectrum of electromagnetic energy. The spectrum that reaches the earth's surface consists primarily of wavelengths between 280nm and 1 mm. To generate these wavelengths for laboratory experiments, Visible (Kodak Medalist II Carousel Projector, Tungsten halogen 35W lamp), UV-A (Q-Panel Co.UVA-340) and UV-B (Spectroline XX-15B) were chosen to mimic natural. The intensity and wavelength of each light source is measured by a calibrated spectroradiometer (Ocean Optics, Inc. USB 2000+ Spectrometer, 3nm bandwidth, 220-890nm with Spectrasuite 1.4.2_09).

The spectroradiometer's irradiance calibration uses a cosine response UV-VIS collector on the input fiber and a lowpass hot mirror filter to prevent longer wavelengths from creating stray light. This instrument has been corrected for nonlinearity and uses the software nonlinear correction feature. Using the calibrated lamp source and Spectrasuite software to create a UV calibration curve and VIS calibration curve, I then merged those into a UV-VIS calibration curve as the measurement reference. The spectroradiometer is installed in a small temperature controlled chamber to reduce variations in response due to temperature fluctuations.

Optical bandpass filters at 510 nm, 460 nm, and 410 nm were chosen for visible light, 390 nm, 370 nm, and 330 nm for UVA light, and 289 nm for UVB light. The number represents the bandpass filter's central wavelength and the measured spectrum for bandpass filter showed the filter has a bandwidth of ~15 nm. The measured width for the passing light is wider than the 10 nm claimed by the Edmund Optics Inc. The

specification for bandwidth is to measure width at 50% of maximum (=Full Width at Half Maximum or FWHM). Through the rest of the document, each treatment is named according to a filter's nominal bandpass wavelength (e.g. visible light passing through 510 nm filter will be called 510 nm solution).

2.2 Experimental Design

Experimental solutions are equilibrated and exposed in cylindrical quartz vessels [40ml, 2cm (diameter) x 15cm (height)]. The top of the quartz vessel is sealed with a Teflon lined cap and two transfer ports. The inlet transfer port is attached to a constant flow air inlet system with an air purifier (DRIERITE, Laboratory Gas Drying Unit L68 NP 303 filled with activated carbon). All quartz vessels are pre-cleaned with 10% hydrochloric acid and rinsed 5 times with deionized water before experiment. The vessel outer sides are covered with aluminum foil and installed in plastic chambers with optical bandpass filters (Edmund Optics Inc.) mounted to the bottom as indicated in Figure 4.

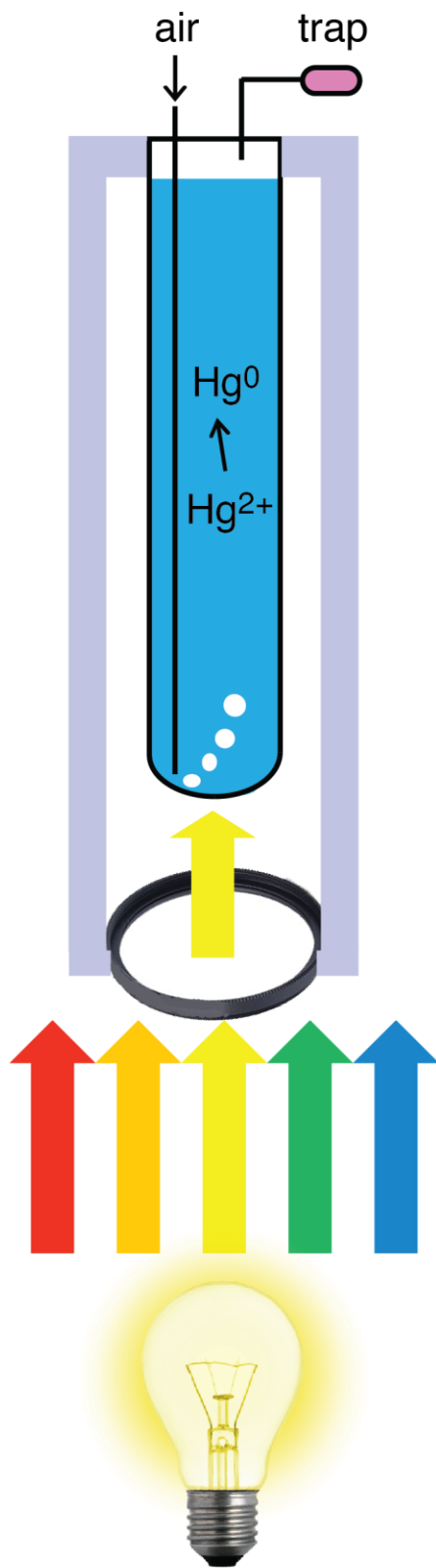


Figure 4. Experimental apparatus for light exposure using optical bandpass filter.

Mercury solutions are diluted from mercury standard (High-Purity Standards, Mercury) and mixed with DOC (IHSS Suwannee River Natural Organic Material (NOM), IHSS No. 1R101N, FL, USA or Nordic Reservoir NOM, Skarnes, Norway, IHSS NO. 1R108N) solution. The mix solutions would be leaved idle to equilibrate for 24 hours before light exposure. The total mercury is 4 ug/L (ppb) while DOC concentration is 6.34 mg/L (ppm) for Suwannee River solution and 11.1 mg/L (ppm) for Nordic Reservoir solution (measured by a Shimadzu Total Organic Carbon Analyzer). The mixed solution is then purged with Hg-free purge gas in an environmental chamber at a temperature of 25°C for two hours in the dark to remove existing DGM before light exposure.

After purging in the dark, the mixture solutions are continuously exposed to the light sources. During the light exposure, any DGM that forms in the solution is purged out onto a gold trap by bubbling air at a constant flow rate of 30 ml min⁻¹ (Figure 4). The gaseous mercury samples are collected every 120 minutes. After collecting the DGM, the gold trap is then heated to 45°C with air flow rate of 40 ml min⁻¹ for 10 minutes to evaporate any moisture that may have condensed inside the trap during exposure. Moisture was never observed in the gold coated sand section of the trap – only occasionally at the inlet end of the glass tube. The mercury adsorbed on the gold trap is then purged and trapped on an analytical trap and measured using a cold vapor atomic fluorescence detector (CVAFS) (Tekran 2500) (Figure 5). Light spectra are measured before and after exposure above the optical bandpass filters using a calibrated spectroradiometer. Absorbance of the test solutions are also measured before and after

exposure with a spectrophotometer (Shimadzu UV-1601). The reaction vessels are placed in the constant-temperature chamber for the entire incubation time.

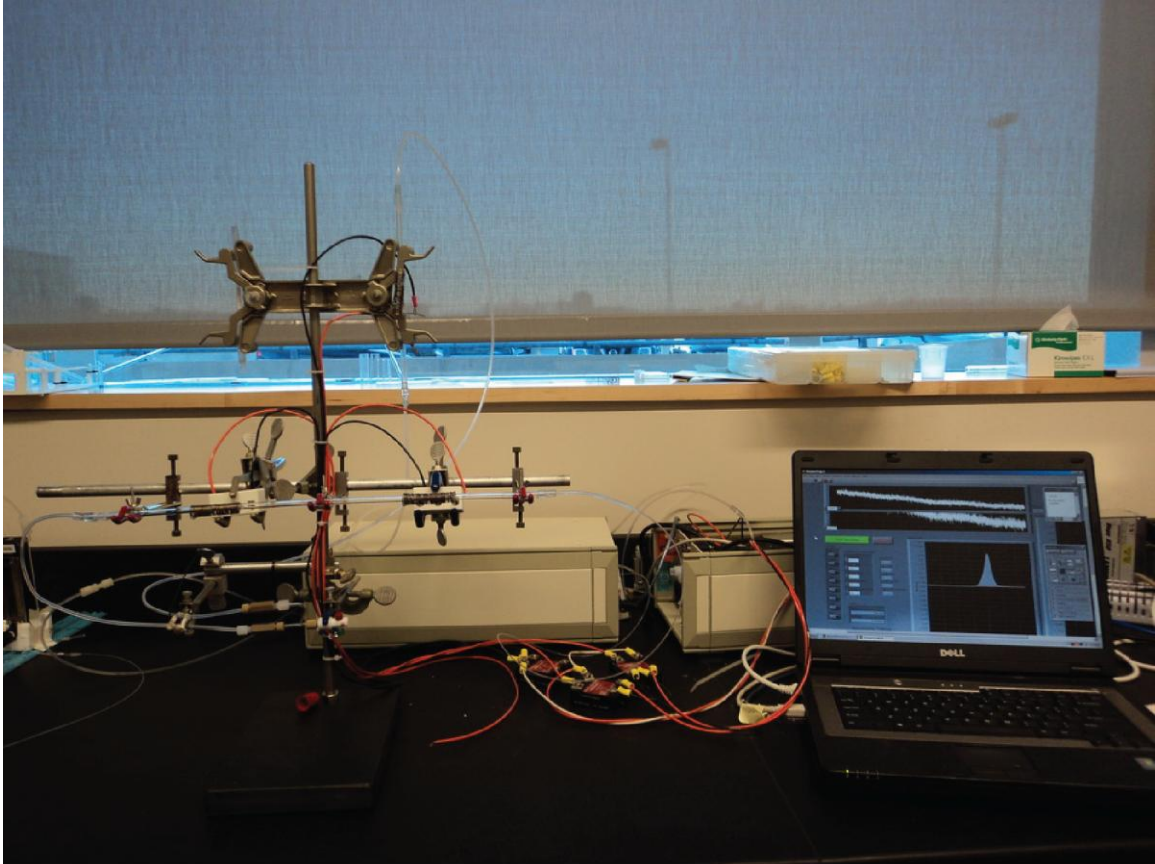


Figure 5. Tekran 2500 cold vapour atomic fluorescence spectroscopy (CVAFS) with mercury injection system and Labview controlling program.

2.3 Absorbed energy over experiment time

Absorbance of the experimental solutions was measured before and after each experiment from 200 to 800 nm in 1nm interval by spectrophotometer. The incident light intensity (I_0) and transmitted light after the solution (I) is calculated for absorbance:

$$\text{Absorbance (OD)} = \log_{10}(I_0/I)$$

The absorbance can be converted to transmittance by the equation

$$\text{Transmittance}_{\lambda} = 1/(10^{\text{absorbance}_{\lambda}(\text{OD}) * \text{optical path length in solution (m)}})$$

where the optical path length in the experimental chamber is 15 cm. After calculating transmittance for each wavelength, absorptance can be acquired by

$$Absorptance_{\lambda} = 1 - Transmittance_{\lambda}$$

The rate of absorbed energy was calculated using the incident light intensity multiplied by the absorptance at the same waveband using

$$Rate\ of\ absorbed\ energy\ r_{Ea}\ (mW/cm^2\ s) = Absorptance_{\lambda} * Incident\ light\ intensity\ (mW/cm^2\ s)$$

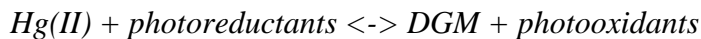
Finally, the absorbed energy for each solution was calculated using the following equation:

$$Absorbed\ energy\ Ea\ (mW) = r_{Ea}\ (mW/cm^2\ s) * T\ (s) * exposure\ area\ (cm^2)$$

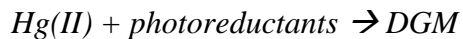
Where T is the exposure time for light exposure.

2.4 Mercury kinetic equation

The overall production of DGM can be described in the following way (O'Driscoll et al., 2004):



Because DGM is being removed immediately after production in this experiment, the reaction can be rewritten as:



Assuming this reaction is pseudo first order reaction, the equation for mercury flux is

$$d[DGM]/dt = kr [Hg(II)]$$

where kr is the rate constant for photoreduction.

2.5 Excitation Emission Matrices (EEMs)

Dissolved organic carbon is ubiquitous in aquatic systems since it is formed by a wide array of biogeochemical reactions. Understanding the composition, structure, and origin of DOC can help us to explain the chemical reaction involving DOC more clearly. Absorbance properties are one method of characterizing the DOC in the solution and can be easily measured using a spectrophotometer. Fluorescence also provides a way to examine how the molecules in DOC behave when excited by specific wavelengths of light. When an electron of molecule absorbs energy and is excited to higher quantum state, because the electron is not stable in the excited state, it then relaxes to its ground state quickly, emitting fluorescence. Because the excitation and emission wavelength are specific for particular molecule, it's easy to characterize the composition by the fluorescence information. Fluorescence is measured by spectrofluorometer (Shimadzu PC-5301), and three dimensional excitation emission matrices (EEMs) can be acquired by adding a series of fluorescence emission spectra by continuously varying excitation wavelengths (Lochmuller et al. 1986; Coble et al 1990). All the EEMs were corrected for inner filter effects and standardized to quinine sulfate equivalent intensity following the methods of Osburn et al. 2011. Different peak areas in the EEMs can be identified and characterized by comparing the excitation/ emission value. We use parallel factor analysis (PARAFAC), one of the popular methods to identify DOC origin, functional groups, complexation with other molecules, etc. Overall, we can use EEMs to identify

fluorescent moieties that would interact at wavelengths of interest, and also use EEMs to examine any changes over time during experiment.

3. Results

3.1 DGM production under different light sources and optical bandpass filters by using Suwannee River NOM

Cumulative DGM production as a function of both wavelength and time are shown in Figure 6. With two hours dark purging, the solution demonstrated nearly zero DGM formation for 20 minutes, indicating that all the existing DGM in the solution had been purged out of solution and there was little or no mercury reduction at the beginning of the light exposure. All three sets of data collected over 8 hours of irradiation showed stable and continuous increase in DGM formation over time. Of the 8 different wavelengths tested, the 289 nm solution generated the highest DGM production at almost all times. The average production over 8 hours was 4000 pg (n=3) for the 289 nm solution, which accounts for about 2.9 % of total 140 ng Hg contained in each 35 mL experimental vessel. The 330 nm solution produced the second highest DGM, in which the 8-hour average was 3000 pg and accounts for 2.1 % release of all the mercury in solution. The 370 nm and 390 nm solutions produced 2100 and 1400 pg over the incubation time and accounts for 1.5 % and 1 %, respectively, of total mercury in solution. For visible light data, the DGM production was smaller than UV light data. The 410 nm and 460 nm solutions showed a similar pattern with both average 1000 pg mercury production over the experiment time. The 510 nm solution showed almost identical results as the dark

solution in three rounds of experiments with the average of 700 pg DGM production. The cumulative DGM showed that DGM production increases with decreasing wavelength.

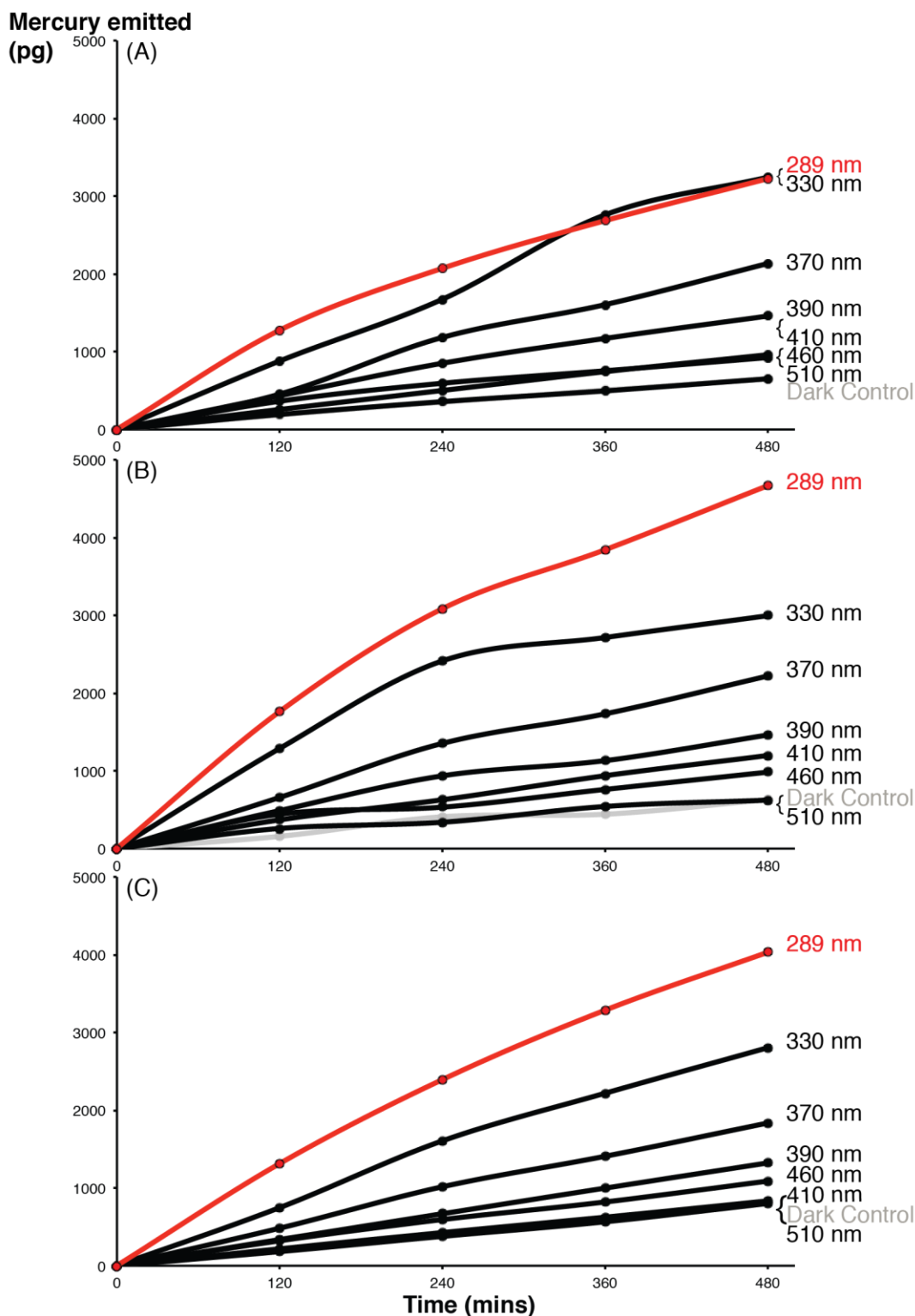


Figure 6. Cumulative DGM production over 8 hours light exposure using different optical bandpass filter with Suwanee River NOM (DOC 6.34mg/L) and Hg 3.96 ug/L. (A), (B), and (C) represent 3 rounds of experiments under the same condition settings. Red line represents the solution underwent the shortest wavelength of light exposure and grey line represents the solution in dark control.

The averaged transmitted light intensity measured after the optical bandpass filters ranges from 115 mW/cm² s to 11400 mW/cm² s (Figure 7) with 289 nm filter having the lowest transmitted light intensity and visible light with 510 nm filter having the highest transmitted light intensity. UVA with different filters have about the same range of energy with UVB with 289 nm filter. Visible light passing through filters has much higher transmitted light intensities than UV lights. On the other hand, absorbed energy, ranges from 16 W to 455 W over 8 hours exposure, doesn't show as much difference as transmitted light between visible and UV light. Generally speaking, the absorbed energy increase as the filter wavelength increases. However, the 460 nm solution is an exception, it absorbs the greatest energy at all times.

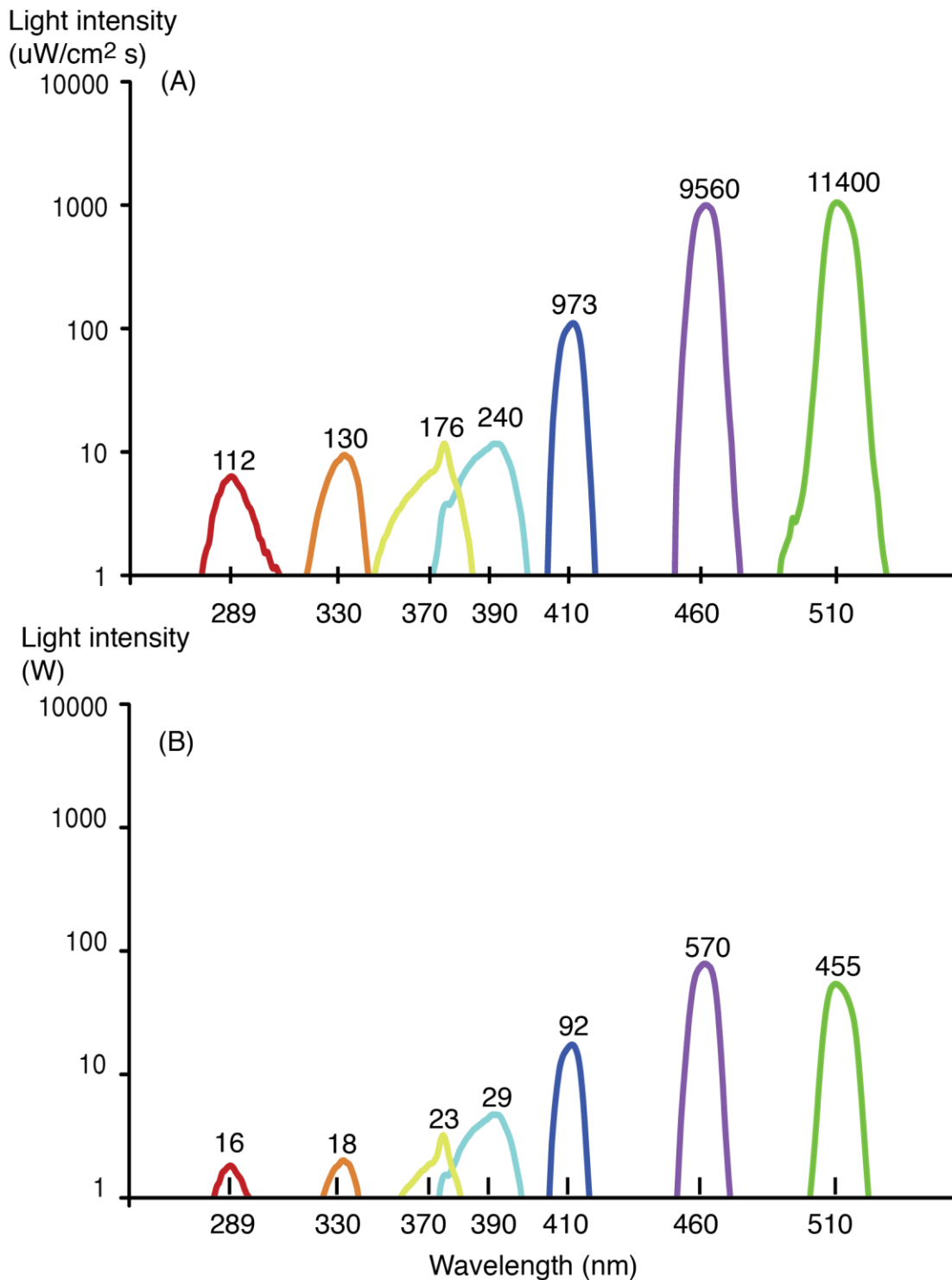


Figure 7. Suwanee River DOC solutions' (A) transmitted light irradiance measured for UVB, UVA, or VIS lamps through bandpass filters, and (B) absorbed light intensities calculated by values in "A" times absorptance, fraction absorbed, and exposure time.

3.2 DGM production under different light sources and optical bandpass filters using Nordic Reservoir NOM

Two rounds of experiments using Nordic Reservoir NOM were collected and exhibited in Figure 8. Similar to Suwannee River DOC solution, both sets of data revealed DGM formation continuously increasing over 8 hours of the experiment. The 289 nm solution again generated the highest DGM at all times with the 8-hour average of 8200 pg (5.9 % of total 140 ng Hg in solution). The other solutions showed almost the same trend as the Suwannee River solution, but only 460 nm solution is an exception (Table 1). The 460 nm solution produced 4100 pg and 5600 pg DGM for each round of experiment and the DGM were higher than 410 nm, 390 nm, and 370 nm solutions. The possible reason why DGM production for 460 nm solutions are higher than UVA solutions will be discussed in next section. Dark solution showed consistently the lowest DGM production for both rounds. The cumulative DGM showed that DGM production increases with decreasing wavelength over time (with only 1 exception- 460 nm filter solution).

Table 1. DGM production and percentage of total mercury in the solution.

| DOC type and concentration (mg/L) | Total Hg (ng/L) | Light source | Filter central wavelength (nm) | Cumulative DGM (pg) | DGM Standard Error | DGM production over total mercury in the solution (%) |
|-----------------------------------|-----------------|------------------------------|--------------------------------|---------------------|--------------------|---|
| Suwannee 6.34 | 4000 | Dark ^{average} | | 700 | 60 | 0.5 |
| | | Visible ^{average} | 510 | 700 | 55 | 0.5 |
| | | Visible ^{average} | 460 | 1000 | 48 | 0.7 |
| | | Visible ^{average} | 410 | 1000 | 110 | 0.7 |
| | | UVA ^{average} | 390 | 1400 | 46 | 1 |
| | | UVA ^{average} | 370 | 2100 | 120 | 1.5 |
| | | UVA ^{average} | 330 | 3000 | 130 | 2.1 |
| | | UVB ^{average} | 289 | 4000 | 420 | 2.9 |
| Nordic 11.1 | 4000 | Dark ^{average} | | 2200 | 270 | 1.6 |
| | | Visible ^{1st round} | 510 | 2200 | | 1.6 |
| | | Visible ^{1st round} | 460 | 4100 | | 2.9 |
| | | Visible ^{1st round} | 410 | 3400 | | 2.4 |
| | | Visible ^{2nd round} | 510 | 3200 | | 2.3 |
| | | Visible ^{2nd round} | 460 | 5600 | | 4 |
| | | Visible ^{2nd round} | 410 | 3800 | | 2.7 |
| | | UVA ^{average} | 390 | 4400 | 300 | 3.1 |
| | | UVA ^{average} | 370 | 4900 | 210 | 3.5 |
| | | UVA ^{average} | 330 | 6700 | 310 | 4.8 |
| | | UVB ^{average} | 289 | 8200 | 730 | 5.9 |

By using different DOC sources, we can observe that UV wavelengths produce higher DGM compared to visible wavelengths. The averaged transmitted light intensity measured after the optical bandpass filters are about the same for UVA and UVB light. A replacement lamp installed before Nordic Reservoir DOC's 2nd round experiment produces a higher intensity of visible light than the previous lamp. The transmitted and absorbed energy for each light source and solution are shown in Figure 9. The transmitted light ranges from 112 mW/cm² s to 40000 mW/cm² s, and absorbed energy ranges from 15 W to 910 W over 8 hours exposure. Absorbed energy show that UVA solutions have almost identical absorbed energy with 289nm solution. The 460 nm solution, like previously results observed for the Suwannee River solutions, still absorbs about the largest absorbed energy among all the solutions. Generally speaking, the absorbed energy increases as the filter wavelength increases.

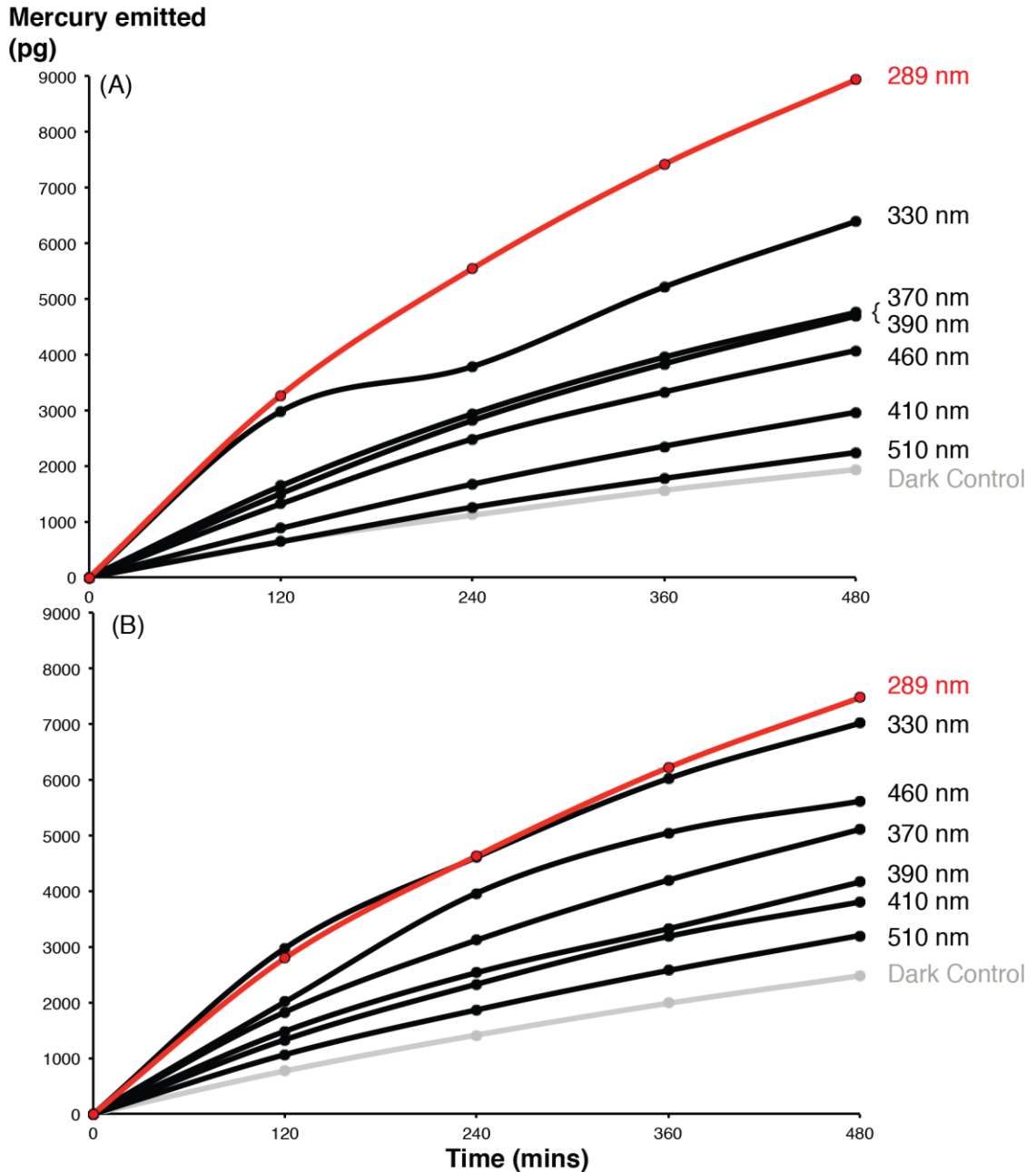


Figure 8. Cumulative DGM production over 8 hours light exposure using different optical bandpass filter with Nordic Reservoir NOM (DOC 11.1mg/L) and Hg 3.96 ug/L. (A) and (B) represent 2 rounds of experiments under the same condition settings. Red line represents the solution underwent the shortest wavelength of light exposure and grey line represents the solution in dark control.

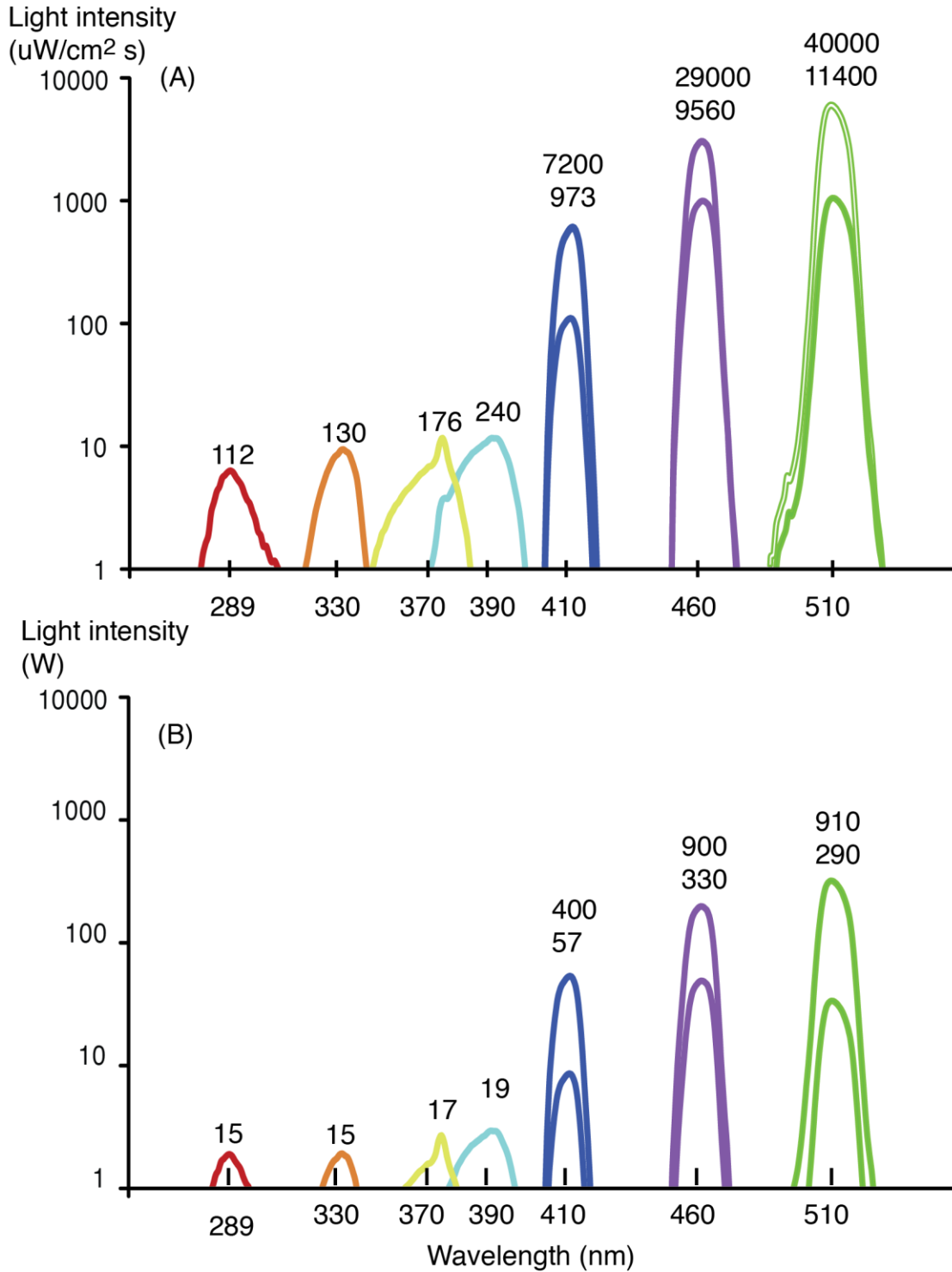


Figure 9. Nordic Reservoir DOC solutions' (A) transmitted light irradiance measured for UVB, UVA, or VIS lamps through bandpass filters, and (B) absorbed light intensities calculated by values in "A" times absorptance, fraction absorbed, and exposure time. Visible light was changed before the second round and thus had two values.

3.3 DGM production over absorbed light

Since the transmitted and absorbed energy are different for all solutions, it would be inadequate to compare different DGM production without considering how the solution interacts with the light. Therefore, we normalize the cumulative DGM data by calculating the phonetically generated DGM emission per unit of absorbed energy. The DGM production of each solution minus DGM production of dark experiment is divided by the absorbed energy, and thus we got the photoefficiency for all the samples (Table 2). Among all solutions, because the 289 nm solution was able to produce the highest DGM of 4000 and 8200 pg over the 8 hours with the smallest absorbed light, and therefore, its photoefficiency is the highest. Generally, as the wavelength increases, the photoefficiency decreases (Figure 10). This result provides us a stepping-stone for future research to predict mercury emission given a set of optical conditions.

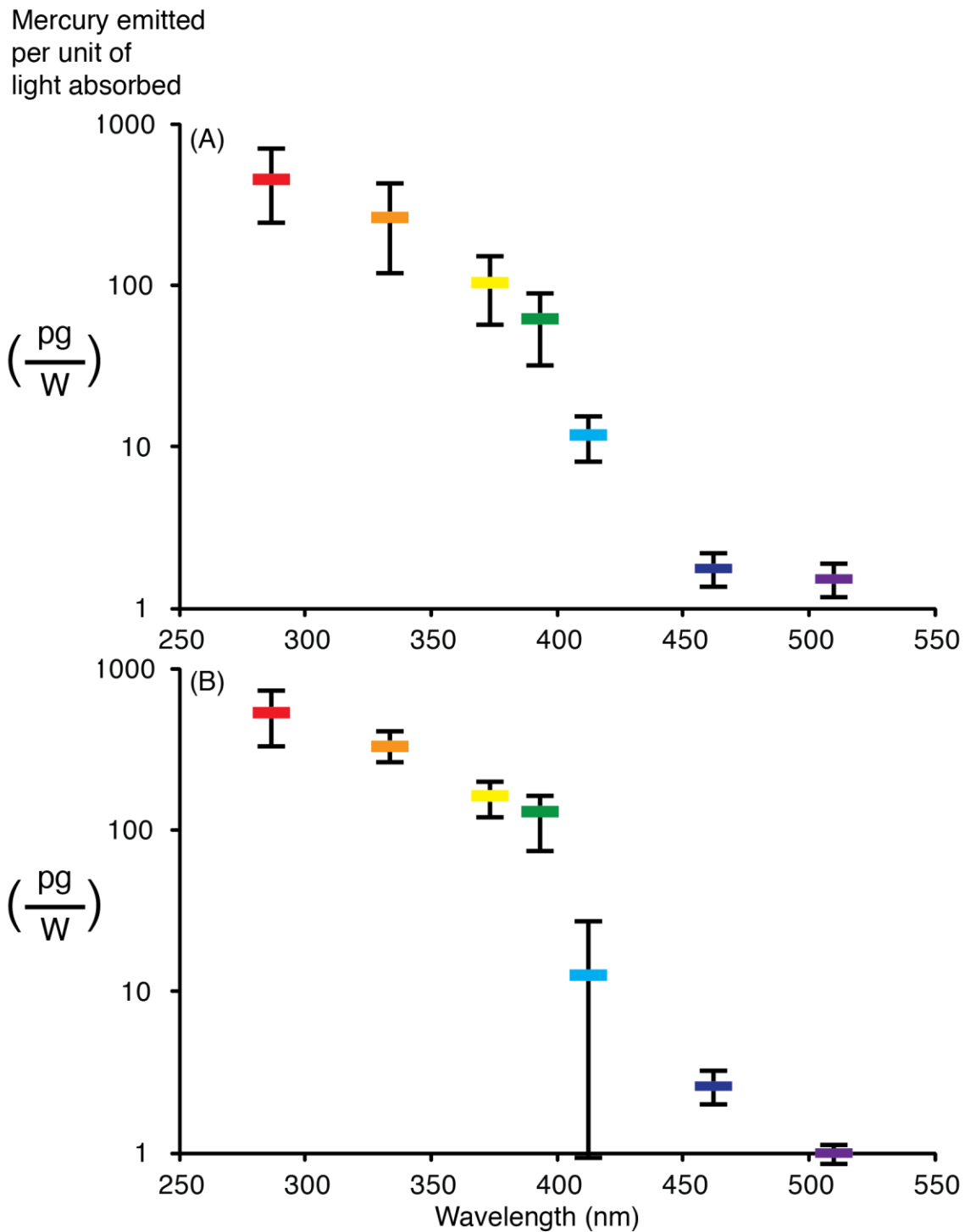


Figure 10. The average photoefficiency (mercury emission over absorbed light) under different filters with (A) Suwannee River DOC solutions and (B) Nordic Reservoir DOC solutions.

3.4 Excitation Emission Matrices (EEMs)

The EEMs for both DOC solutions before and after adding mercury (Figure 11) show two main peaks regions for both solution are near excitation/emission = 250/460 nm (the highest peak) and 325/450 nm (moderate peak). Suwannee River solution had higher peak height than Nordic Reservoir solution while Suwannee River solution's DOC concentration is lower than that of Nordic Reservoir solution. After adding the mercury, both solutions demonstrated the decreasing of both peak heights. Mercury complexation seems to quench the fluorescence in both DOC solutions.

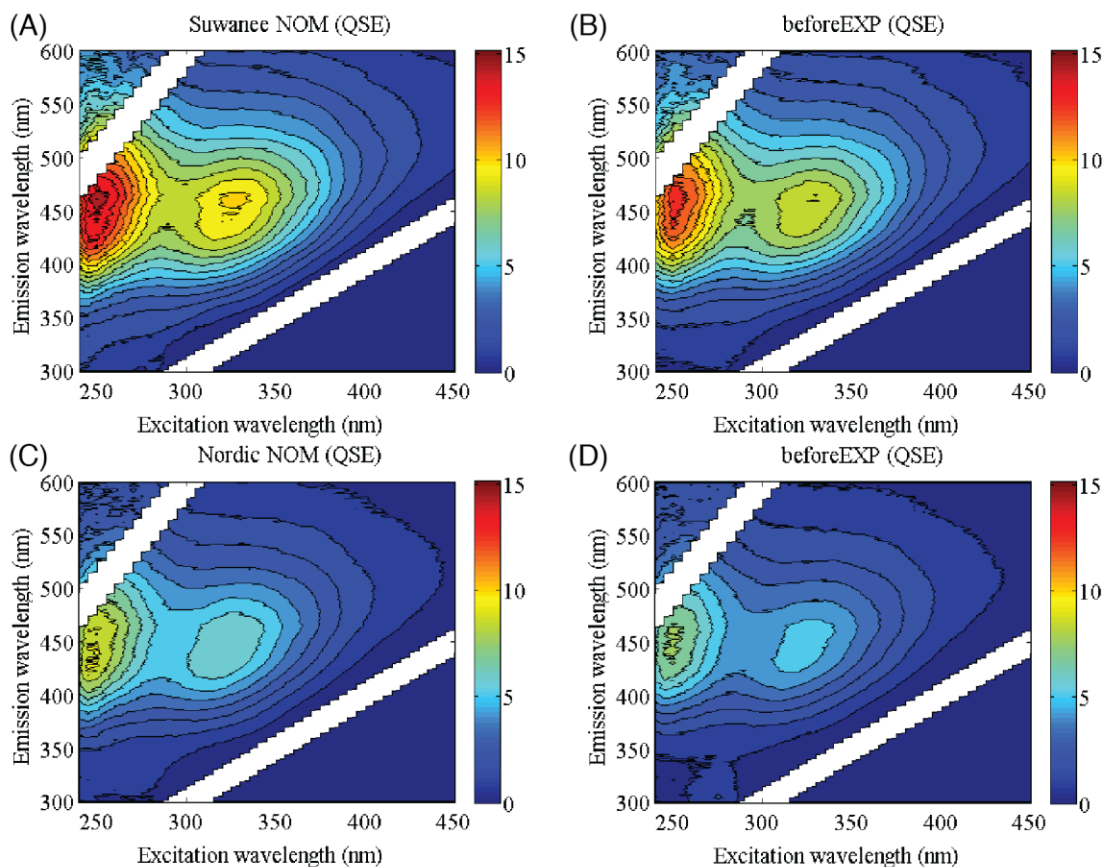


Figure 11. The Excitation Emission Matrices (EEMs) for Suwannee River DOC solution (A) before and (B) after adding mercury. Nordic Reservoir DOC solution (C) before and (D) after adding mercury.

After light exposure, all solutions were measured and displayed in Figure 12 and 13. For Suwannee River solutions, the EEMs seems to increase in 325/450 nm peak area (except 410 nm solution), and the 250/460 nm peak shifted a little to higher emission wavelength and the peak area became a little smaller after light exposure. For Nordic Reservoir solutions, the 250/460 nm peak shifted a little and increased to higher emission wavelength for solutions after experiment. The 289 nm solution exhibited increase in both two main peaks, but all other solutions seems to decrease in the 325/450 nm peak.

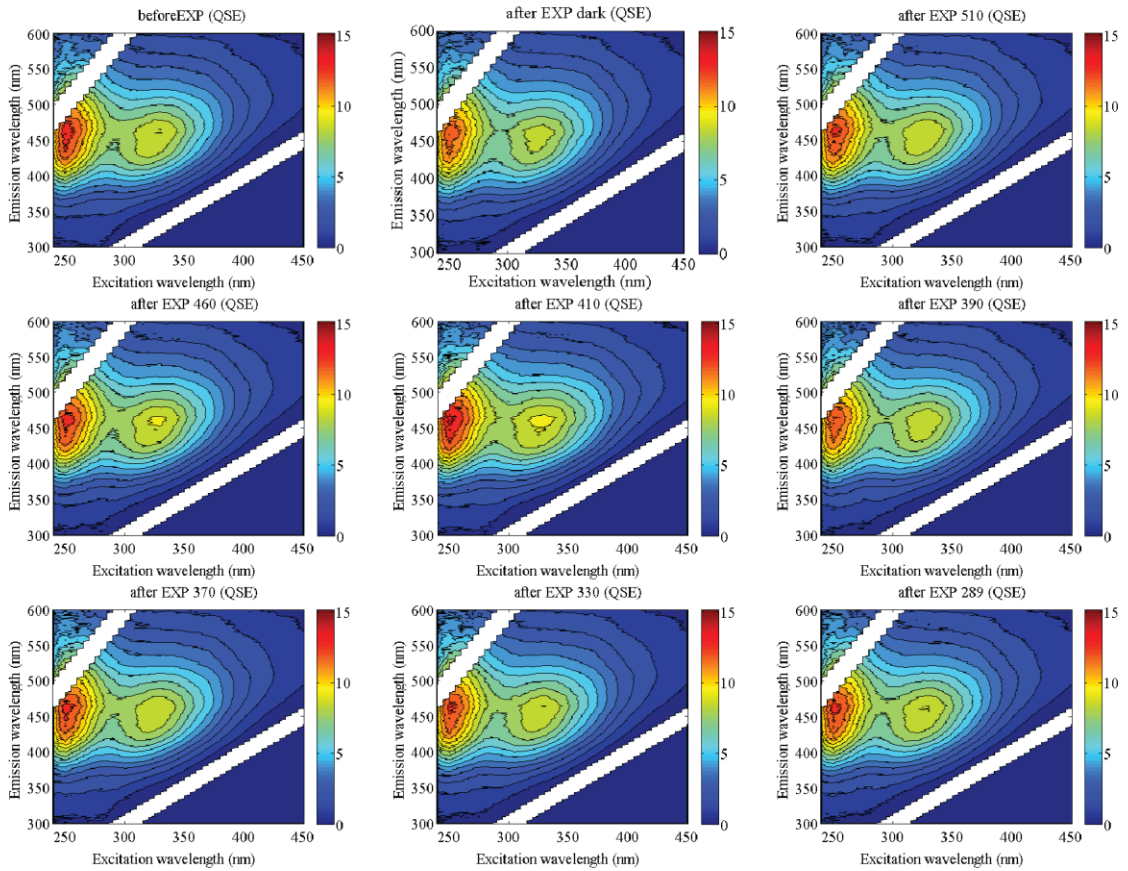


Figure 12. The Excitation Emission Matrices (EEMs) for Suwannee River DOC solution before and after light exposure.

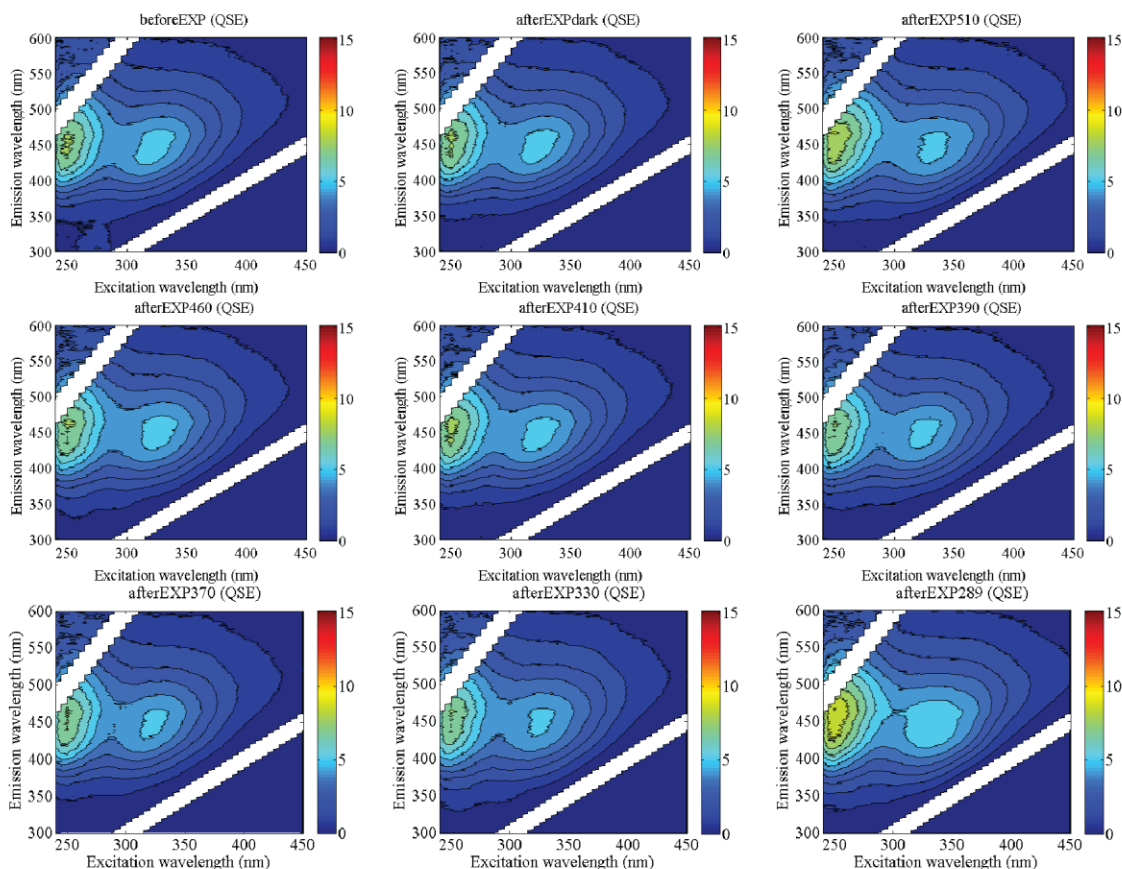


Figure 13. The Excitation Emission Matrices (EEMs) for Nordic Reservoir DOC solution before and after light exposure.

4. Discussion

4.1 DGM emission over time and DGM emission over absorbed energy under different types of light, filters, and DOC sources.

The influence of light on mercury photoreaction can be examined through mercury emission over time (DGM emission rate) and mercury emission over absorbed light, photoefficiency. The total results of all the experiments are shown in Table 2. I shall analyze the data in the following ways (1) DOC role in mercury photoreduction, (2) different light intensities, (3) DGM production rate, and (4) DGM light efficiency.

Table 2. Comparison of cumulative DGM production, DGM production rate and Photoefficiency.

| DOC type and concentration (mg/L) | Total Hg (ng/L) | Light source | Filter central wavelength (nm) | Cumulative DGM (pg) | Absorbed light (W) | DGM production rate (pg/L min) | Photo-efficiency (pg/W) |
|-----------------------------------|-----------------|------------------------------|--------------------------------|---------------------|--------------------|--------------------------------|-------------------------|
| Suwannee 6.34 | 4000 | Dark ^{average} | | 700 | | 42 | |
| | | Visible ^{average} | 510 | 700 | 460 | 42 | 0 |
| | | Visible ^{average} | 460 | 1000 | 570 | 59 | 0.53 |
| | | Visible ^{average} | 410 | 1000 | 92 | 59 | 3.3 |
| | | UVA ^{average} | 390 | 1400 | 29 | 84 | 24 |
| | | UVA ^{average} | 370 | 2100 | 23 | 120 | 61 |
| | | UVA ^{average} | 330 | 3000 | 18 | 180 | 130 |
| | | UVB ^{average} | 289 | 4000 | 16 | 240 | 210 |
| Nordic 11.1 | 4000 | Dark ^{average} | | 2200 | | 130 | |
| | | Visible ^{1st round} | 510 | 2200 | 290 | 130 | 0.12 |
| | | Visible ^{1st round} | 460 | 4100 | 330 | 240 | 5.7 |
| | | Visible ^{1st round} | 410 | 3400 | 57 | 180 | 13 |
| | | Visible ^{2nd round} | 510 | 3200 | 910 | 190 | 0.79 |
| | | Visible ^{2nd round} | 460 | 5600 | 900 | 330 | 3.5 |
| | | Visible ^{2nd round} | 410 | 3800 | 400 | 230 | 3.3 |
| | | UVA ^{average} | 390 | 4400 | 19 | 270 | 130 |
| | | UVA ^{average} | 370 | 4900 | 17 | 290 | 170 |
| | | UVA ^{average} | 330 | 6700 | 15 | 400 | 300 |
| | | UVB ^{average} | 289 | 8200 | 15 | 490 | 400 |

(1) DOC role in mercury photoreduction

Contrary to O’Driscoll’s results in 2003, my testing data showed that there was no lag-time between light exposure and mercury photoreduction. For both DOC solutions, the data showed DGM production for dark solutions are not zero, which means the solution itself reduces mercury without invoking photochemistry. Previous research showed that Hg(II) can be reduced by humic substances in the water (Allard and Arsenie 1991) and oxidation was not obvious in dark solution (Lalonde et al. 2004).

Suwannee River DOC solutions, with lower DOC concentration, had generally lower cumulative DGM production over 8 hours experiment than that of Nordic Reservoir solutions. The DOC concentration of Nordic Reservoir solution is about 75% higher than that of Suwannee River’s solution, however, the DGM production are about 2 to 4 times higher. The DOC in the solution should have enough bonding site for mercury

to complex with because DOC concentration are at least 20000 times higher than mercury concentration (DOC is 0.53 mM for Suwannee River NOM and 0.93 for Nordic Reservoir NOM while mercury is 0.02 μ M). Among all the functional groups in DOC, previous research showed that mercury prefers to complex with DOC's thiol group first (Xia et al. 1999, Hesterberg et al. 2001, Ravichandran 2004, and Skyllborg et al. 2006) and then other functional groups like carboxyl group. Mercury complexed with thiol group would also exhibit higher reduction rate for mercury than the other functional group in DOC (Xia et al., 1999, Hesterberg et al., 2001, Ravichandran 2004, and Skyllborg et al., 2006).

Other researchers report that mercury would mostly bind to the carboxylic functional groups or phenolic groups because these groups are the most abundant in DOC. The thiol group, although has the highest bonding preference for mercury, accounts to very small portion in DOC (Suwannee River NOM has 0.65% (w/w) sulfur content), and thus may not be the most important factor in reducing mercury. The stability constant measured for mercury to complex with the whole humic substance is much lower than the stability constant of mercury to complex with thiol or sulfur containing group (Chai et al. 2012) If this is true, then we can consider all the difference between two DOC solution are mainly from the concentration difference and the most abundant groups' characteristics in the DOC.

According to Haitzer 2002, if Hg/DOC ratio is approximately lower than 1 μ g of Hg/1 mg of DOC, mercury will be bond to DOC strongly. If Hg/DOC ratio is more than 10 μ g of Hg/1 mg of DOC, mercury boding would be weaker. Both sets of Hg/DOC ratios in Table 2 are below 1 μ g of Hg/mg of DOC, but Suwannee solutions' Hg/DOC

ratio was much closer to 1ug of Hg/1mg of DOC ratio, which mean Suwannee solutions should form stronger Hg-DOC bonding and thus should have stronger mercury photoreduction. Nevertheless, the two DOC solutions have about the same order of Hg/DOC ratio, which would probably have similar concentration effect for mercury reduction.

(2) Different light intensities

Because we happened to change the visible light bulb for the last round of experiment, it provided us with a chance to examine the influence of light intensity in the reaction. The new visible light bulb's transmitted light intensities were higher than those of old one. As a result, the absorbed light intensities and cumulative DGM were higher. The transmitted light increase 3 to 7 times higher and the absorbed light increase almost correspondingly, but the cumulative DGM production increased only 12% to 45% more. In 2011, Oh and Kim measured the DGM production rate under three different UVA and UVB light intensity. Oh's data showed that the rise in light intensity would also increase the DGM. In their research, the rise of their UVA light intensity from 0.5 to 3 mW/cm² resulted in cumulative DGM production increment from 4.41 to 7.99 ng/L under 6 hours exposure. Their UVB light intensities rise from 0.02 to 0.2 mW/cm² and their cumulative DGM production increment from 9.78 to 24.79 ng/L for the same period of time exposure.

Therefore, both our data and Oh's showed the stronger intensity of light, the higher the DGM production, but the cumulative DGM production won't increase linearly with light intensity (Figure 14). Our absorbed light intensity provides us a good way to explore this issue. For all three visible light solutions, if we use the old light bulbs of

absorbed/transmitted light intensity ratio to expect the absorbed light intensity using new light bulb, the absorbed light intensity should be higher. The result means that the increasing transmitted light couldn't be absorbed at the same proportion by the solution. Further studies may be conducted to check if all other the small wavelength of light in UV range would follow the same trend showed in Figure 14.

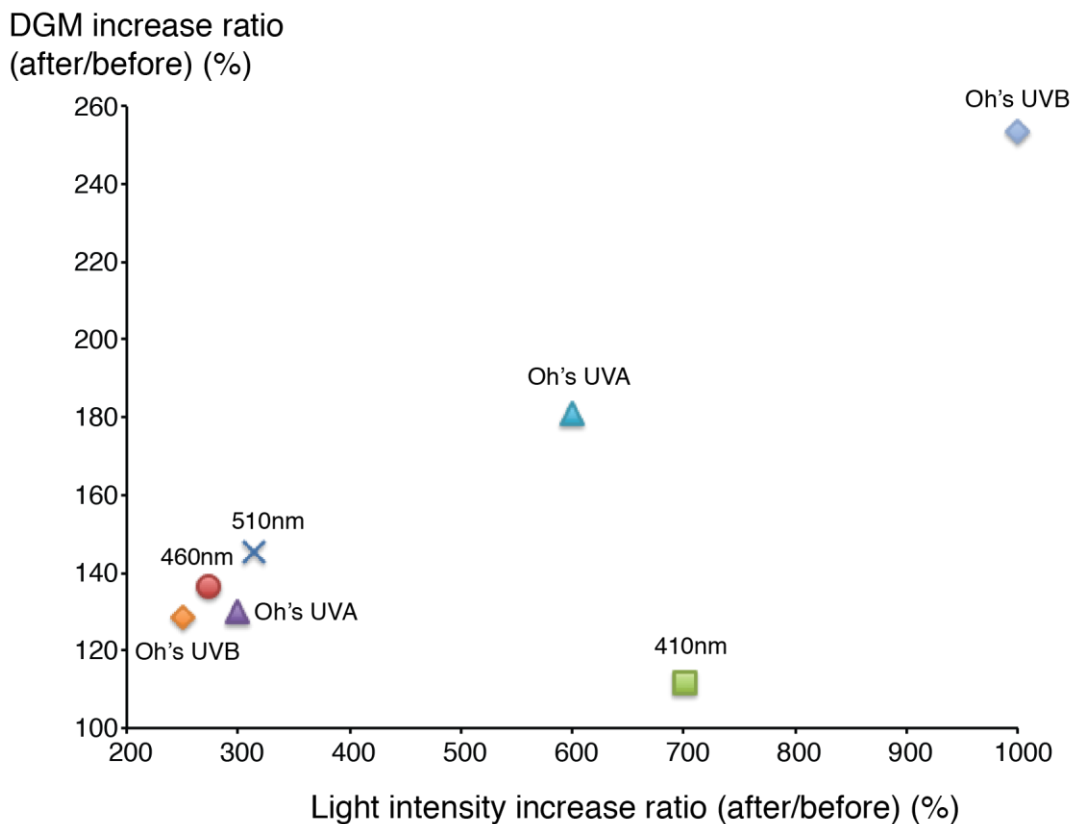


Figure 14. DGM production increase ratio with the increase of light intensity.

(3) DGM production rate

Calculating the cumulative DGM production over solution volume and then dividing the result by 8 hours of exposure time, we can calculate a DGM production rate (Figure 15). As wavelength increases, DGM production rate decreases. The 460 nm solution rate was higher than we would anticipate in the overall trend. From table 2, we

observed that 460 nm solution absorbs almost the highest energy even though 510nm received the highest transmitted light. A previous study found that organic material's light absorption is largely independent of concentration (Stevenson 1994) and the absorption of long wavelength of light (> 350nm) would increase because of intramolecular charge transfer interaction within DOC's hydroxyl-aromatic donors and quinoid acceptors (Del Vecchio and Blough 2004). Del Vecchio used laser light 460 nm and 532 nm and found these lights would results in the solution absorption loss and photobleaching, not only at the laser wavelength but also at 300 nm. From their research, absorption change for SRFA and SRHA (Suwannee River fulvic acid and humic acid, which are the main composition for our Suwannee solution) were similar for 460 nm laser light and 510 nm laser light even the 460 nm light is much weaker than 510 nm light (460nm is 10 mJ/pulse and 510 nm is 532mJ/pulse). This research helps us explain why the 460 nm solutions can absorb the highest light (even though the 510 nm has the highest transmitted light). In addition, it also help us explain why 460nm solutions have higher DGM production and higher DGM production rate than 410 nm, 390 nm and 370 nm solutions in our Nordic solution results. Intramolecular charge transfer interaction enable the DOC to transfer the light energy from the chromophores that are far away from the mercury along with the long carbon chain to mercury binding area and then reduce mercury.

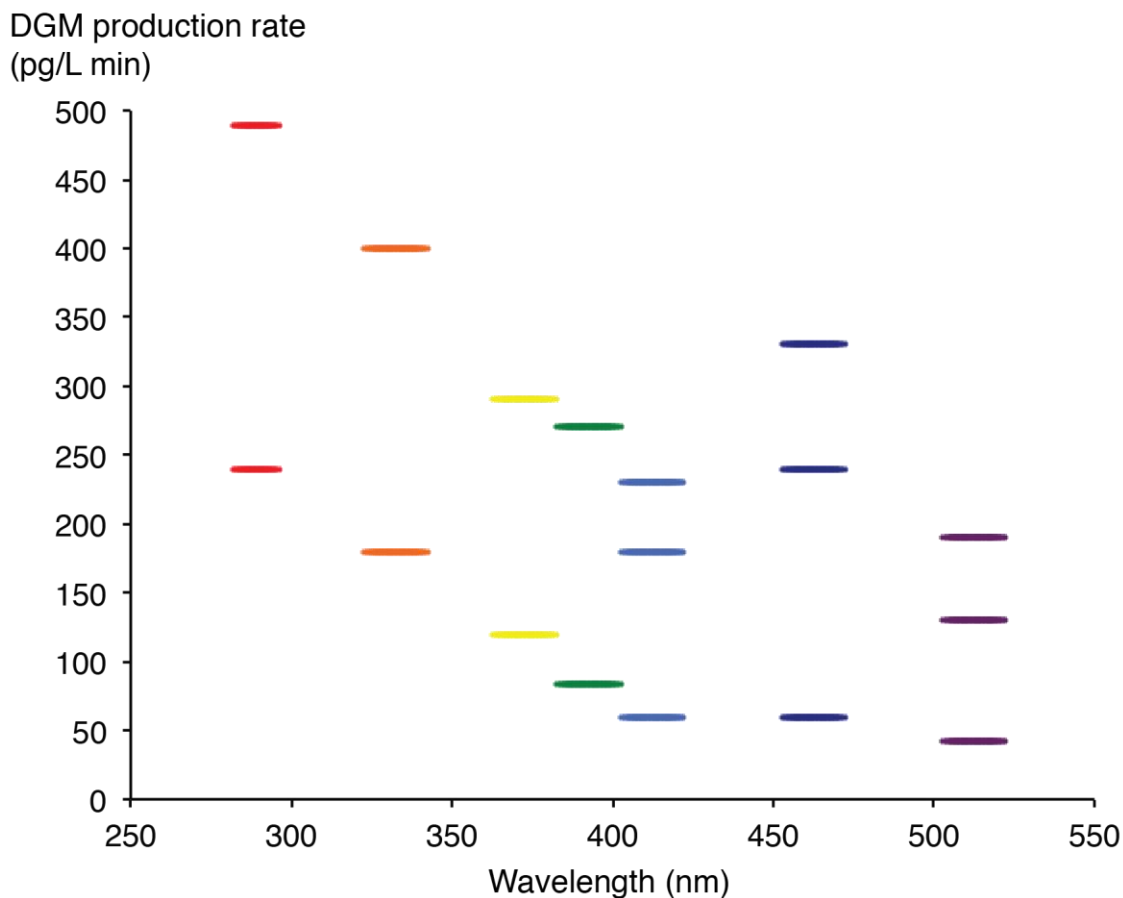


Figure 15. DGM production rate for all data sets.

(4) DGM photoefficiency

DGM photoefficiency increases with the decreasing of light wavelength for both Suwannee and Nordic solution. Our results showed 289 nm solutions have 1-3 orders of magnitude higher DGM photoefficiency than visible light solutions and have about the same or 1 order of magnitude higher than UVA solutions. The Suwannee 510 nm solution doesn't show significant DGM production compared to the dark solution and thus the photoefficiency is 0. It doesn't mean visible light at 510 nm range will not photoreduce mercury, but just because we couldn't differentiate it under the constraint of our detection limits. Nordic Reservoir solutions have a few times higher photoefficiency than that of Suwannee River solutions, which is not proportional to the DOC

concentration difference (75 % increase from Suwannee solution) (Figure 16). The photoefficiency difference between the two DOC solutions becomes larger with the increasing wavelength. Since UVB 289 nm light has the highest photoefficiency and triggers mercury photoreduction most effectively, it might decrease the influence from DOC concentration. On the other hand, the longer the wavelength lights are not as strong as UVB in reducing mercury, and the DOC structure and concentration would be a more important controlling factor. Other possibilities include the stronger absorption of UVB or the binding site of mercury compared to chromophore.

Increasing the light intensity for Nordic Reservoir solutions results in the decrease of 460 nm and 410 nm solutions' photoefficiency but increase of 510 nm solution's photoefficiency. Apparently, increased light intensity should decrease the photoefficiency from our previous discussion that the higher transmitted and absorbed light won't reveal in the increase of DGM production accordingly. For the 510 nm solution, a possible explanation might be because the original 510 nm photoefficiency is too low and the increase of light finally increases the DGM production enough to be measurably higher than the dark solution.

Oh's data also showed that UVB has a higher light efficiency than UVA (calculating the DGM production over light intensity). Because Oh's water samples were collected from South Korean field sites, it would be inappropriate to use our absorbance to calculate absorbed energy for them. Amyot et al. (1997a and b) concluded that UVB accounts for 64-97% of total DGM production in Arctic lakes under low DOC concentration. Both of these results agree with our conclusion that UVB has higher photoefficiency than UVA and visible light.

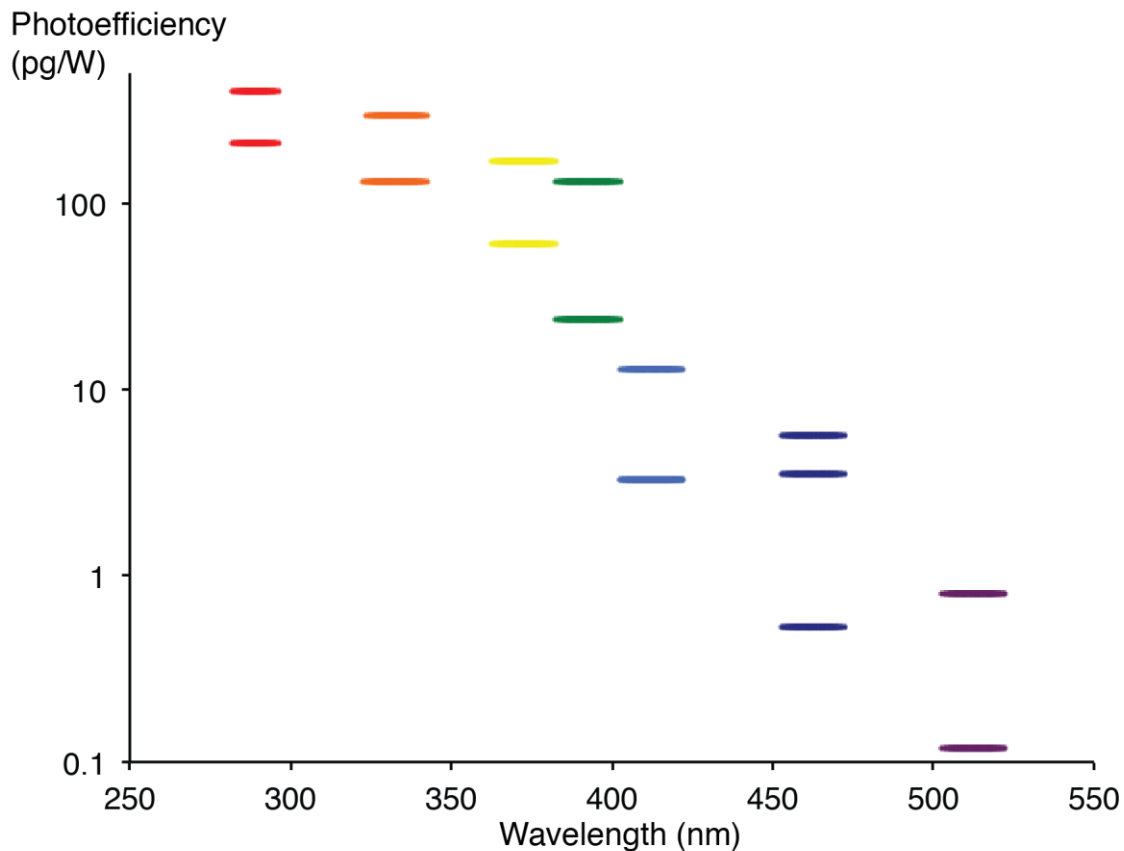


Figure 16. Photoefficiency for all data sets.

4.2 Relationship between DGM production and DOC absorbance change

Since mercury binds to DOC in the water and undergoes photoreduction, measuring DOC absorbance can provide more clues for DOC characteristics and light's influence. Figure 17 compares the pre-exposure DOC solution and post-exposure 289 nm solution to examine the difference due to light exposure. The DOC absorbance remains almost constant above spectrum of 400 nm and increases at wavelengths in the UV range. DOC absorbs UV light more effectively than the visible light spectrum and thus has larger capability to transfer energy to the sorbed mercury. This explains despite the low intensities of UV lights, UV light can still produce more DGM than visible lights. On the other hand, even though 510 nm solutions absorb 2 orders of magnitude higher energy

than UVB, most of the absorbed energy is not sufficiently transmitted to regions where the photobleaching occurs, and thus where the mercury reduction occurs. From Figure 17, we can also observe two things: first, the Suwannee River solution absorbance is higher than Nordic solution. Because Suwannee DOC concentration is lower, we then know Suwannee NOM can absorb considerably more light per unit of carbon and Suwannee might have higher densities of chromophores per unit of carbon. Secondly, the Nordic Reservoir solution underwent greater absorbance change than Suwannee River solution, which hinted that Nordic Reservoir is more susceptible to photobleaching. There is no research that proves the bleaching would result in the mercury reduction, but the electron release when bond breakage then reduce the mercury can be thought as a possible way to connect the greater absorbance change in Nordic Reservoir samples and mercury reduction. The absorbance change helps us explain why Nordic Reservoir can have higher DGM production and photoefficiency per unit of DOC concentration of Suwannee River DOC.

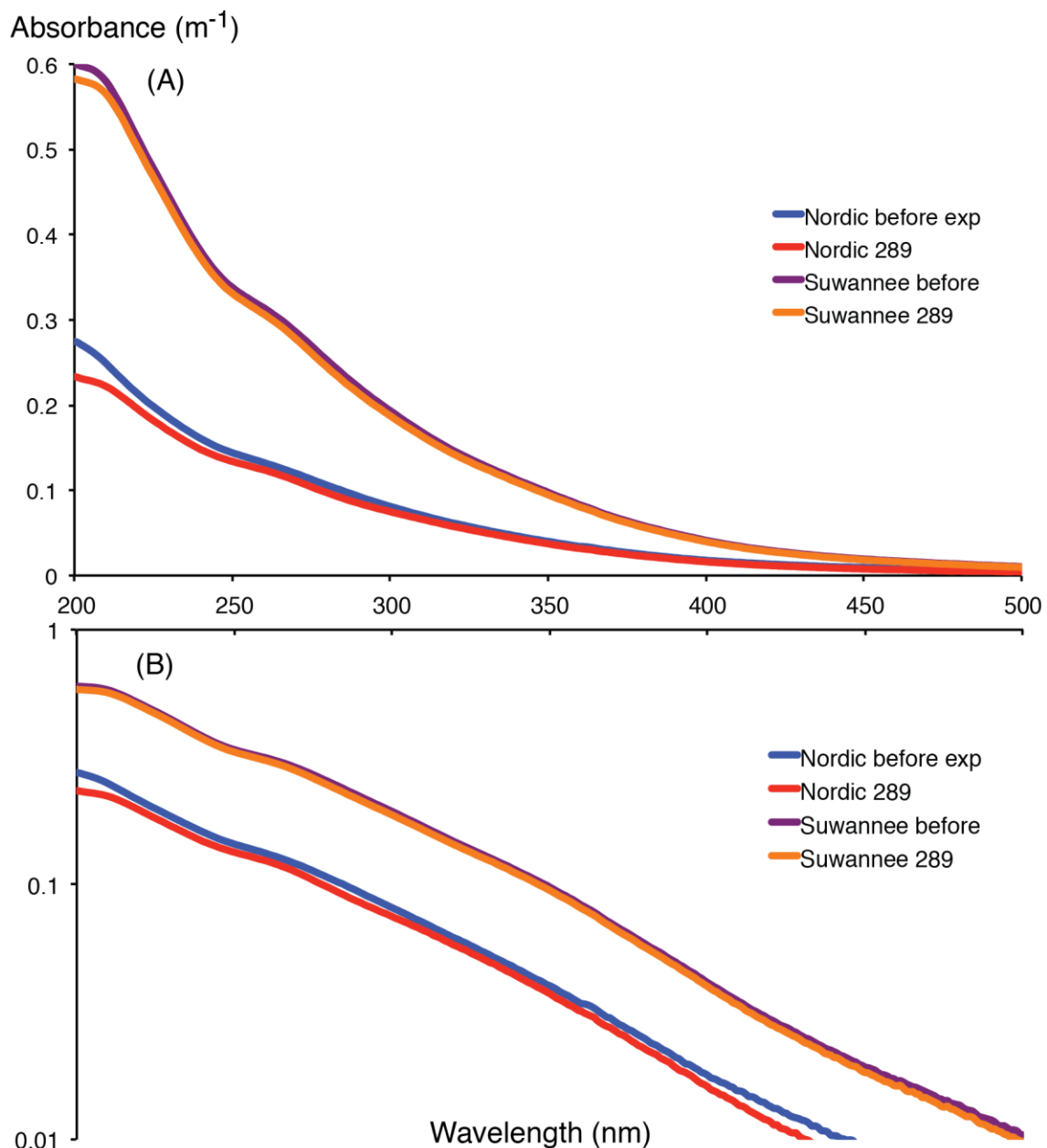


Figure 17. Absorbance change for two DOC solutions. (A) in normal scale and (B) in logarithm scale in y-axis.

Calculating the change in absorbance due to the light exposure, we can explore the magnitude of absorbance change as a function of exposure wavelength (Figure 18). The 289 nm and 330 nm solutions had the highest absorbance change for both DOC solutions. The 460 nm solutions had the 2nd or 3rd highest absorbance change, that supports why 460

nm solutions would have higher DGM production than 410 nm and 390 nm solution. The higher absorbance change indicates 460 nm was bleached more by higher absorbed energy and intramolecular charge-transfer interaction.

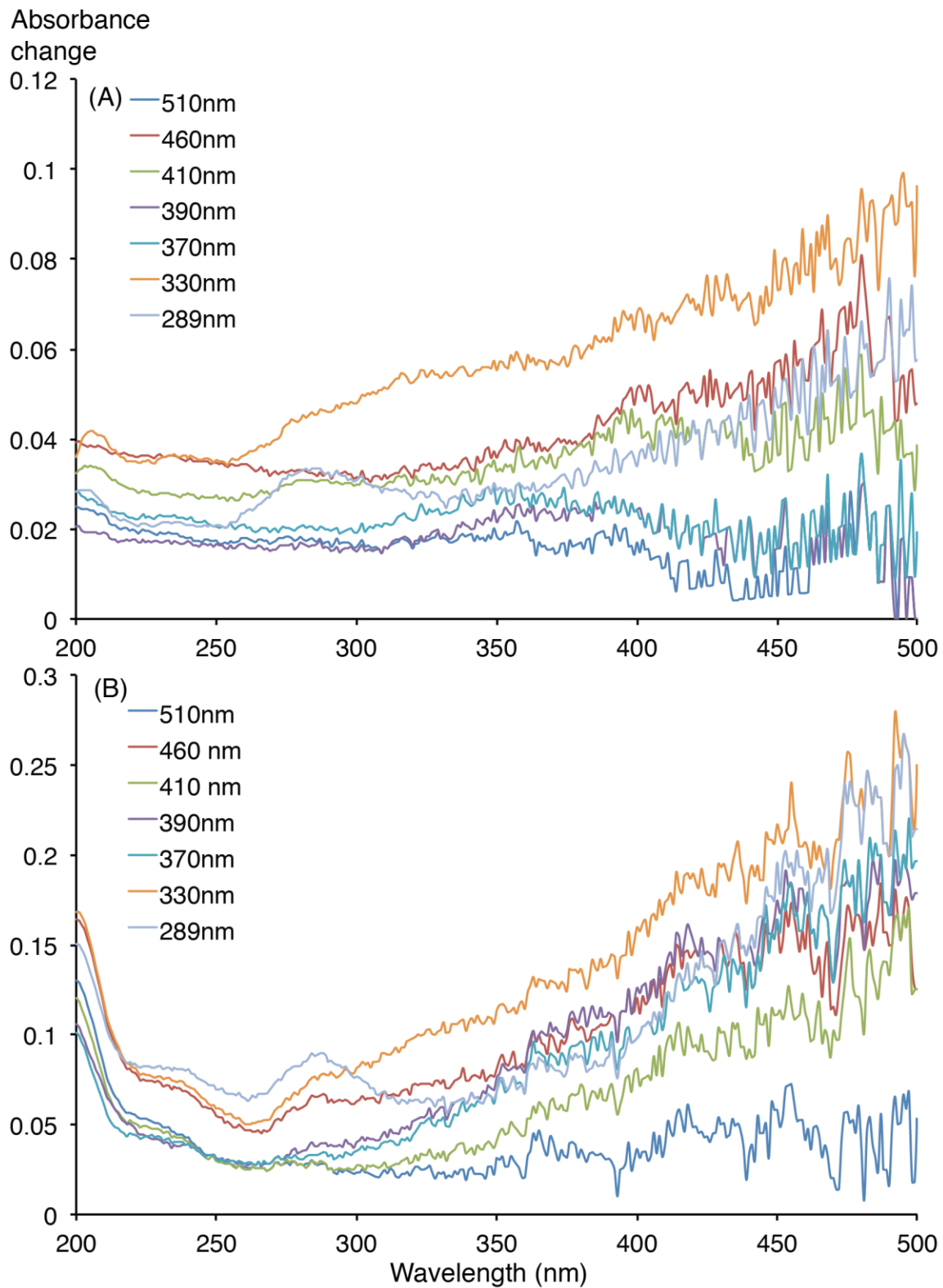


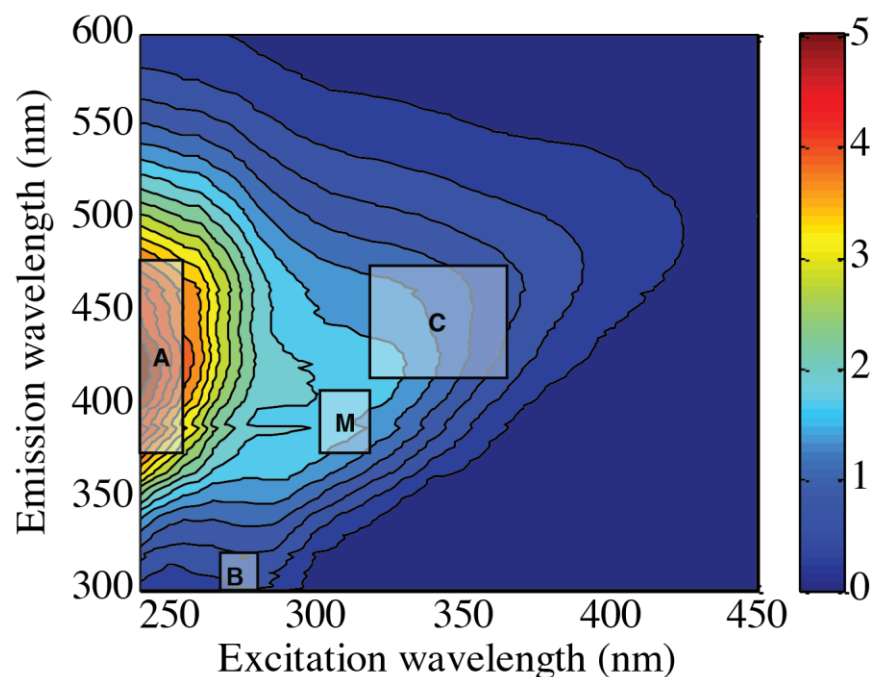
Figure 18. Absorbance change (1-fraction of original absorption). (A) Suwannee River DOC solutions. (B) Nordic Reservoir DOC solutions.

4.3 Excitation Emission Matrices (EEMs)

Parallel factor analysis (PARAFAC) is used to identify the fluorescent component in the DOC. Research has identified the positions of the most common fluorescent moieties in the DOC on an EEM (Ishii et al. 2012, Fellman et al. 2010, Stedmon 2003, and Coble 1996). Table 3 lists the related peak location in the EEMs that were confirmed in the previous studies. Comparing the component peak location, Suwannee River and Nordic solutions are dominated by A and C peaks, which represent terrestrial humic substances originating from vascular plants. The Nordic Reservoir solution before experiment showed a very small B peak (aromatic amino acid) but the peak disappeared after light exposure for all solutions. Since the initial peak is very small, we can't be sure that the Nordic Reservoir contains amino acid.

Table 3. Major fluorescent peaks of aquatic DOC in the EEMs.

| Peak | Excitation (nm) | Emission (nm) | |
|------|-----------------|---------------|--|
| A | 260 | 380-460 | UVC terrestrial humic. High molecular weight and aromatic humic. |
| B | 275 | 310 | Tyrosine (aromatic amino acid) |
| C | 320-360 | 420-460 | UVA terrestrial humic. High molecular weight humic. |
| M | 312 | 370-410 | UVA marine humic. |



Suwannee River humic acid (SRHA) has two main peaks at 261/457 nm and 325/452 nm while Suwannee River fulvic acid (SRFA) has two main peaks at 245/445 nm and 320/443 nm (Her et al. 2003). The DOC composition will have positive correlation with the EEMs' peaks existence, however, we don't know if the concentration of certain functional group would also have linear relation with the peak values. For the following discussion, we assumed the function group would influence the peak height in proportion with their quantity in the DOC. Because our Suwannee River NOM seems to have a higher peak at the emission wavelengths for humic acid (261/457nm), we suspect that Suwannee River NOM has higher portion of humic acid than fulvic acid (Figure 19).

Other studies have also presented EEMs pattern for Nordic Reservoir fulvic acid and humic acid (Mobed et al 1996). Their EEMs demonstrate Nordic Reservoir fulvic acid would have peak at 320/450 nm and 360/470 nm and Nordic humic acid would have peak at 300/470 and 370-410/470-490 nm, and our Nordic Reservoir NOM seems to be more similar with their fulvic acid. Hence, our Nordic Reservoir NOM contains more fulvic acid than humic acid, and Suwannee River NOM is the opposite.

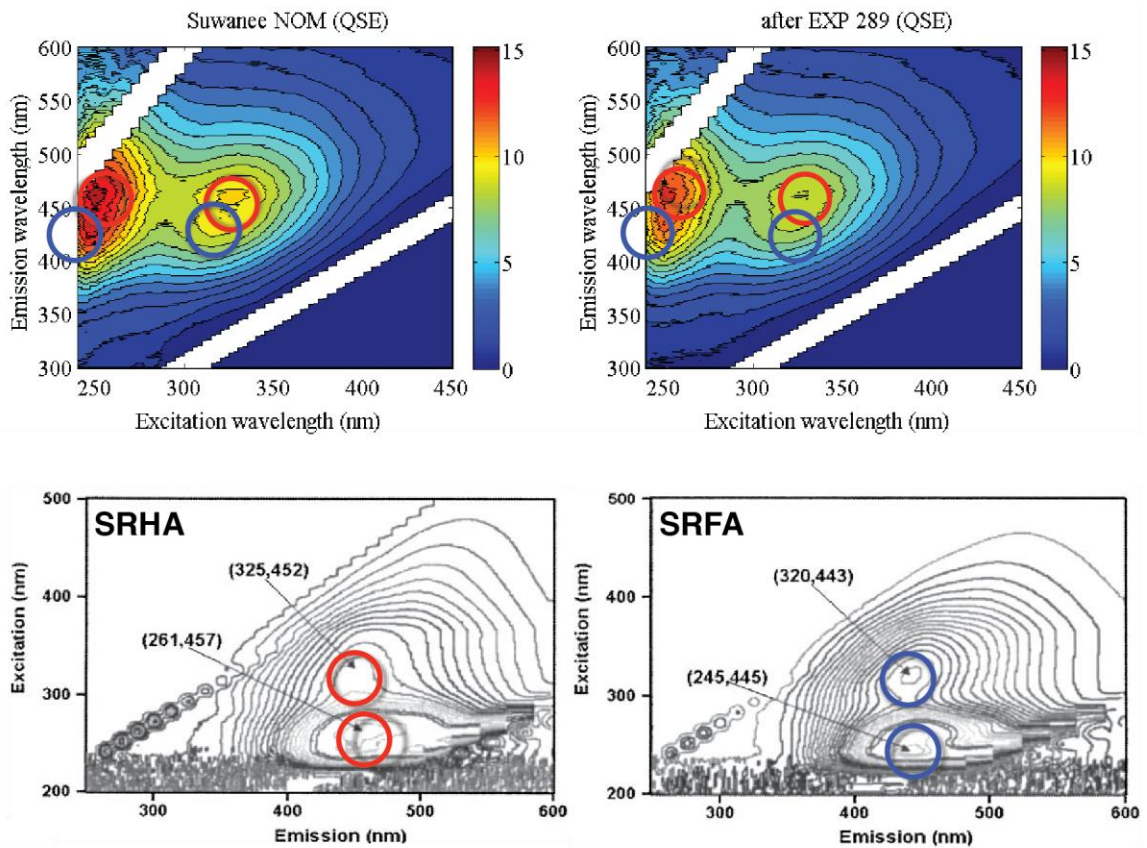


Figure 19. Suwannee River NOM solution EEM compared with Suwannee River Humic Acid (SRHA) and Suwannee River Fulvic Acid (SRFA).

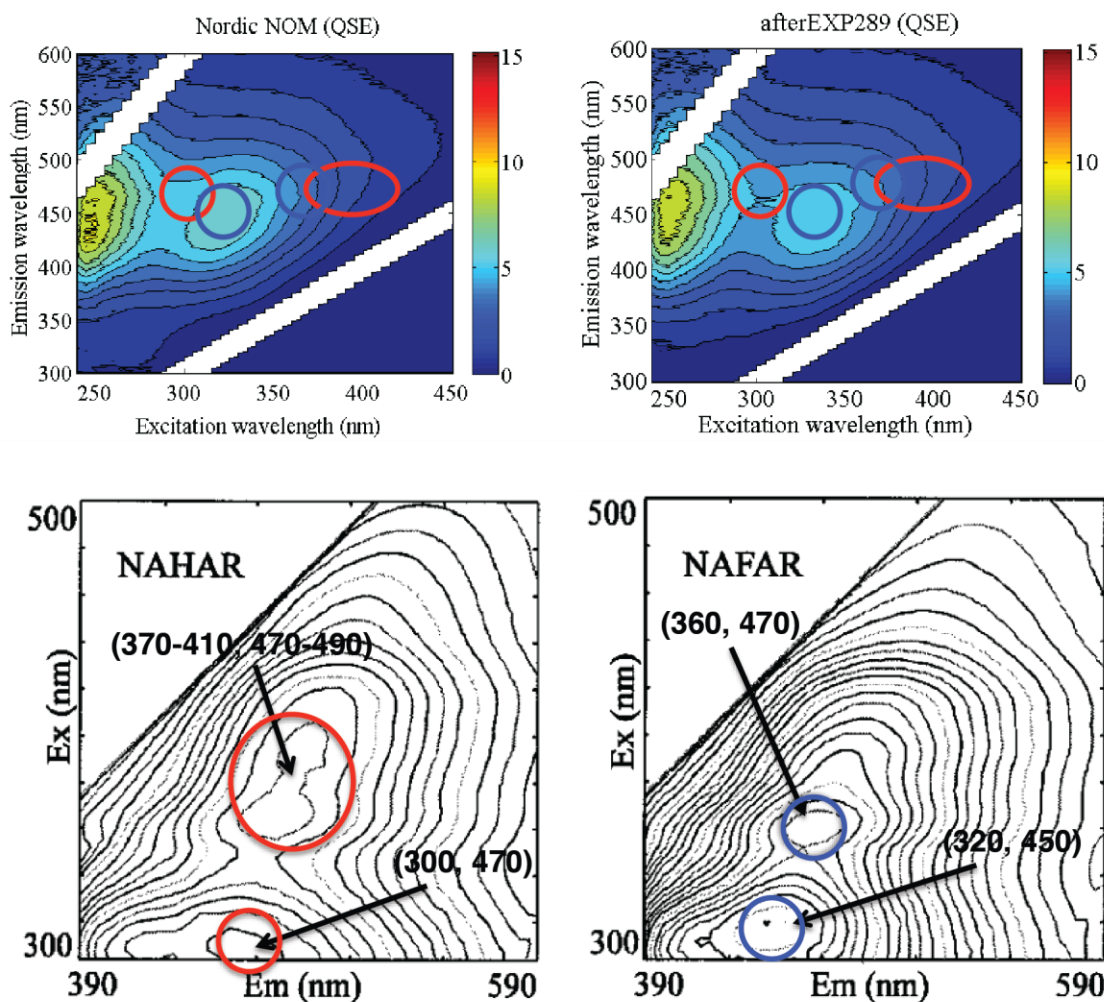


Figure 20. Nordic Reservoir NOM solution EEM compared with Nordic Reservoir Humic Acid reference (NAHAR) and Nordic Reservoir Fulvic Acid reference (NAFAR).

The functional group's difference might contribute a portion effect other than DOC concentration in DGM production. Significant fluorescence decreases in the EEMs were observed when mercury complex with the DOC (Chai et al. 2012), and our EEMs also showed a fluorescence decrease after adding mercury to the two DOC solutions. Chai pointed out that fulvic acid, having higher carboxylic group ratio, has much higher mercury complexing capacity and stability constant than humic acid. Combining Chai's conclusion that fulvic acid is more important in complex with mercury and our finding

that Nordic Reservoir solution has higher fulvic acid while Suwannee has higher humic acid, we hypothesize that the reason why our Nordic solution increase DOC concentration 75% but can increase DGM 2 to 4 times higher is because Nordic Reservoir NOM contains higher fulvic acid content. The explanation for DOC composition by examining the EEMs should later be evaluated by other methods to test this hypothesis.

4.4 DGM kinetic rate constant

Both Qureshi et al. 2010 and O'Driscoll et al. 2006 had DGM pseudo first order rate constant k_r values for around 0.15- 0.93 h^{-1} . Our results show k_r ranges from 2.19×10^{-5} to $2.7 \times 10^{-4} \text{h}^{-1}$. The reason why our k_r values are 3 to 4 orders of magnitude lower than previous data might have two explanations. First of all, our original reducible mercury is 3 orders of magnitude higher than their natural ocean, river, or lake waters. Previous research observed DGM production plateau in DGM production graph, but our DGM emission seemed still to increase steadily. During our experiment time, we only photoreduced a small portion of mercury in the solution, and thus our k_r are all small. Secondly, the lights they use are all wide band of UVA and UVB light while we are using a small fraction of UVA and UVB light. Our testing experiments (see supporting information) demonstrate that UVA and UVB light without filter would produce higher DGM. The rate constant k_r , which doesn't take into account the light intensity but only calculating the total mercury in solution and DGM production over time. Thus, rate constant would be higher for wider band spectrum of light than narrow wavebands of light.

4.5 Predicting natural condition by using photoefficiency calculations

From the experimental results, we obtained photoefficiency values for light ranges from 289 nm to 510 nm. It would be an exciting test if we can use our result and apply it to predict natural water mercury emission by combining a best fit for photoefficiency trend with incident solar information. The two DOC solutions we used are natural organic material (NOM), which are derived from natural waters and thus the characteristics should not be too different than other DOC existing in other water bodies. There were two fit curves for Nordic Reservoir solutions because Nordic Reservoir solutions' visible lights were different. We originally used power and exponential trendline to fit the photoefficiency curve because the light absorption by DOC is believed to have exponential increase when decreasing wavelength. However, the photoefficiency values differ greatly in UV and visible light range might suggest the photoefficiency would not behave similarly in these two regions. We can observe in the exponential and power fit curve light near 200 nm would have 5 orders of magnitude higher photoefficiency than light near 400 nm, and these discrepancy among the different spectrum might not reveal the real condition. Therefore, two separate linear trendlines were applied to the photoefficiency in UV and visible range. RTBasic (Biospherical Instruments Inc.) was used to model the specific date's solar irradiation. The ozone layer information for certain date in the model is obtained from NASA Total Ozone Mapping Spectrometer website. The estimated DGM production is calculated by solar irradiance intensity at that date times the fitted photoefficiency curve (Figure 21).

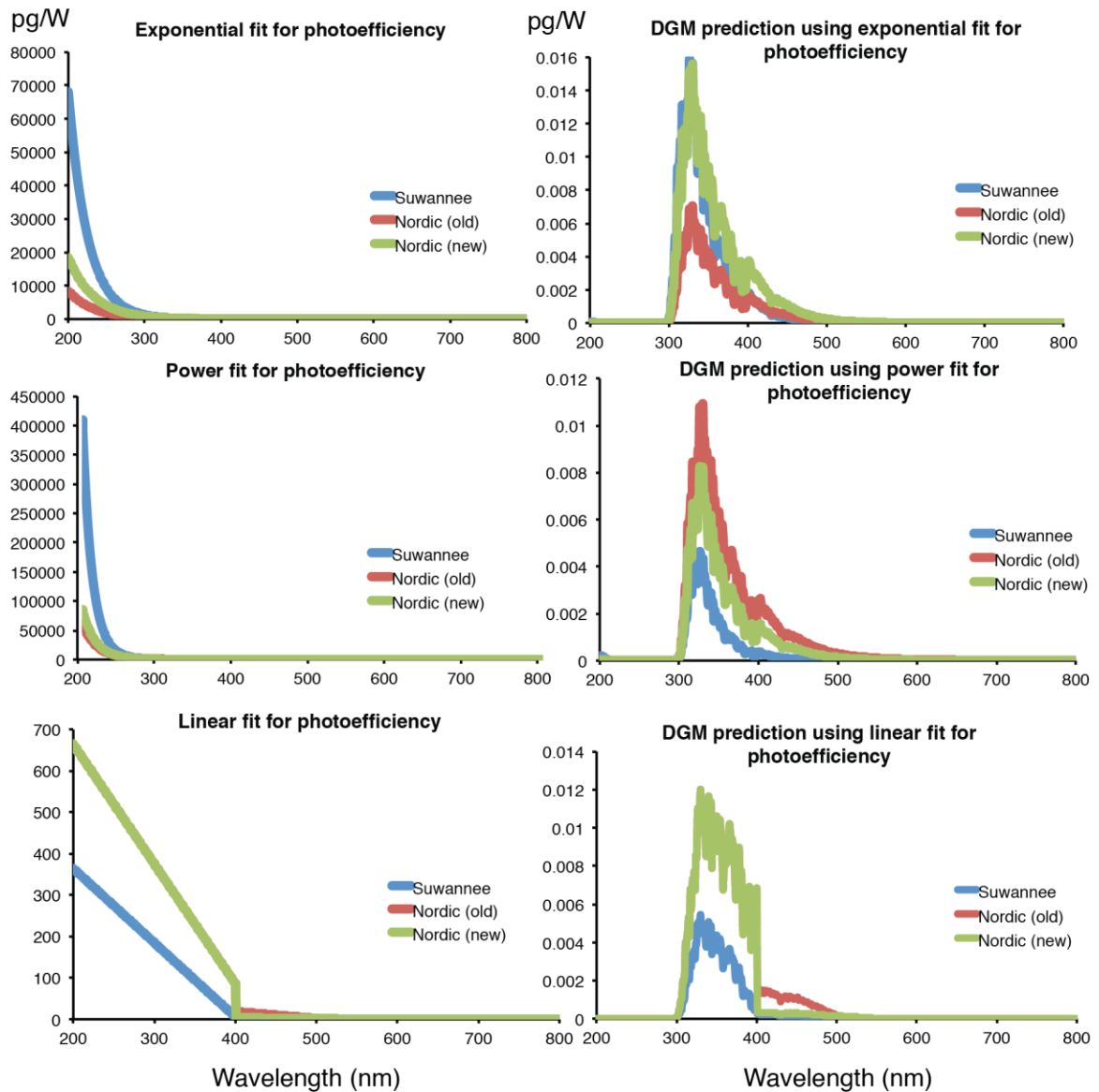


Figure 21. Photoefficiency fit curve and predicting DGM production.

There are three main factors that would influence DGM production when we collected data: mercury concentration, light source type and intensity, and DOC type and concentration. To make our model easy to compare with previous data, I simplified the situation by the following assumption. First, I assume all types of the DOC behave similarly for different water columns and the DGM production is proportionally related to the DOC concentration. Second, I assume the DGM production would have linear

relation with the mercury concentration in solution. The first assumption is created because we haven't had a good way to quantify different DOC in the model at this point. The second assumption is necessary since the mercury concentration in our solutions was considerably higher than natural waters. I compared our predicting DGM values with measured DGM values from Lake Giles, PA (Peters et al. 2007). Since our solutions have extreme high mercury and DOC, linear adjustment for our predicted data are shown in Table 4. Peters showed 1.5 mg/L DOC treatment solution had DGM emission values ranged from 0.8 to 2.3 ng/m² h, while our prediction ranges from 1.37 to 4.42 ng/m² h for exponential fit model, 1.23 to 2.19 ng/m² h for power fit model, and 1.11 to 1.81 ng/m² h for linear fit model. For 2.5 mg/L DOC treatment, their data ranged from 0.19 to 2.5 ng/m² h and our prediction ranges from 2.28 to 7.37 ng/m² h for exponential fit model, 2.05 to 3.65 ng/m² h for power fit model, and 1.85 to 3.02 for linear fit model.

Table 4. Photoefficiency model apply to the same situations with Peters et al. 2007 research.

| Photoefficiency fit method | model prediction (ng/m ² h) | Adjustment [Mercury] to 1.8 ng/L | Adjustment [DOC] to 1.5 mg/L | Adjustment [DOC] to 2.5 mg/L |
|----------------------------|--|----------------------------------|------------------------------|------------------------------|
| Exponential | | | | |
| Suwannee | 41500 | 18.7 | 4.42 | 7.37 |
| Nordic (old) | 22500 | 10.1 | 1.37 | 2.28 |
| Nordic (new) | 49900 | 22.4 | 3.02 | 5.04 |
| Power | | | | |
| Suwannee | 11500 | 5.19 | 1.23 | 2.05 |
| Nordic (old) | 36000 | 16.2 | 2.19 | 3.65 |
| Nordic (new) | 25000 | 11.2 | 1.52 | 2.53 |
| Linear | | | | |
| Suwannee | 10500 | 4.70 | 1.11 | 1.85 |
| Nordic (old) | 30000 | 13.4 | 1.81 | 3.02 |
| Nordic (new) | 27000 | 12.4 | 1.67 | 2.78 |
| Peters et al. 2007 | | | 0.8-2.3 | 0.19-2.5 |

The exponential fit model all seems to predict higher values than that of power fit and linear fit model, but we can't conclude the exponential fit curve is wrong since our parameter to make the model are not comprehensive. We need more accurate adjustments combining like mercury concentration, DOC structure and concentration. The linear fit curve seems to reveal the true condition more precisely with only one data locates out of the real value range. Consequently, with only a few conditions we possess to create the model, linear fit model might be the best solution to predict the real situation.

Our model also showed that the DGM emission mostly originates from UVA range while UVB produces very small portion of DGM. The reason is because ozone layer attenuates most UVB, and thus almost no UVB reaches the ground. We know from our previous results that UVB can produce the highest mercury emission, but in natural condition, UVA, with the strong photoefficiency and relative bigger amount quantities, accounts for the majority part of DGM production.

Overall, our predictions are very close to natural DGM production value, and the reason would because we consider the two most important factors: light and DOC. More parameters, like halogen, pH, other dissolved ions, temperature, will need be consider to later making this model more accurate. All the model calculation will be provided in the supporting information.

5. Conclusion

DGM productions from Suwannee and Nordic DOC solutions had been examined by using three light sources with optical bandpass filter. The DGM production increases as the wavelength decreases for most of the experiments (460 nm solution using Nordic

DOC is the only exception). DGM production normalized by absorbed light showed the photoefficiency, which increases at shorter wavelengths. This study provides the first calculation of photoefficiency for discrete wavebands from 289 nm to 510 nm. The 289 nm solution possessed the highest photoefficiency and this result helps to solve the existing question whether UVB is the most important trigger in mercury reduction.

Evaluation of light absorbance revealed that visible light passing through 460 nm had the highest absorbed energy and 3rd highest absorbance change, which is the result of intramolecular charge transfer interaction within DOC's hydroxyl-aromatic donors and quinoid acceptors. This finding explained why 460 nm light produces higher DGM than smaller wavelength of visible light and some UVA lights. The excitation emission matrices (EEMs) demonstrate that the DOC solutions are composed of terrestrial humic-like material and the solutions underwent little changes over 8 hours light exposure. Using parallel factor analysis (PARAFAC) to compare our EEMs with previous EEMs, we recognize that Nordic Reservoir NOM contains higher concentration of fulvic acid and thus have greater capability to complex with mercury. The structure difference, aside from DOC concentration, makes Nordic Reservoir NOM have higher mercury reduction ability than Suwannee River NOM.

Finally, utilizing the best fit of photoefficiency and solar irradiation information, we can create a model to predict DGM production in certain date. The model can predict values that are closed to the previous record values by only considering two factors. However, our model is still too simplified and is just a stepping stone for future research. More parameters and adjustment will need to be considered to make the model more comprehensive and applicable to predict different natural water columns.

Chapter 3. Supporting information

The results shown in the Chapter 2 are the most important emphasis of this research. Nevertheless, lots of information such as light sources' spectrum, DGM production and photoefficiency for every two hours, Excitation Emission Matrices peaks values, and model calculation would be presented here. Some testing DGM production under different mercury and DOC concentration and the predicting model calculation would also be included.

3.1 Light source spectrum

All the light sources were measure by USB 2000+ spectroradiometer, and all the sources displayed a broad band of spectrum (Figure 20). If we didn't utilize optical bandpass filter, then we couldn't make solid conclusion for each light since they all contain a portion of other light sources.

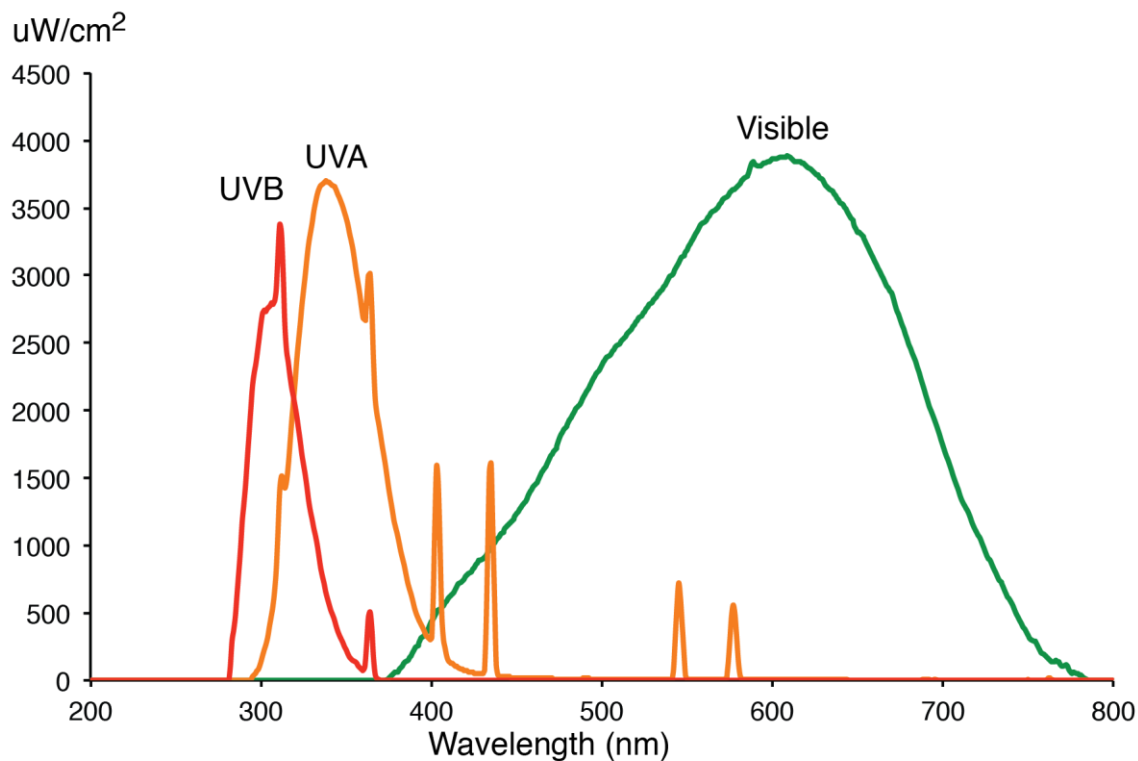


Figure 22. Light source spectrum for UVB, UVA, and visible light.

3.2 Detailed DGM production, absorbed energy, and photoefficiency discussed in Chapter 2.

Four datasets for each round of DGM collected for each set of experiment were listed in Table 5. DGM production would generally be highest in the first 2 hours and then the emission would decrease over time. We only measured solution absorbance after 8 hours exposure, but since there is no large difference after light exposure, I used the end absorbance to calculate the absorbed energy for 2 to 6 hours dataset. We also can observe the photoefficiency is normally highest in the beginning two hour and would decrease over time.

Table 5. DGM production for all experiments.

| DOC type and concentration (mg/L) | Light source | Filter central wavelength (nm) | Cumulative DGM production | | | | |
|-----------------------------------|----------------|--------------------------------|---------------------------|--------------|--------------|--------------|------|
| | | | 2 hours (pg) | 4 hours (pg) | 6 hours (pg) | 8 hours (pg) | |
| Suwannee 6.34 | Dark | | 190 | 350 | 500 | 650 | |
| | Visible | 510 | 190 | 360 | 500 | 650 | |
| | Visible | 460 | 360 | 600 | 750 | 920 | |
| | Visible | 410 | 260 | 500 | 740 | 960 | |
| | UVA | 390 | 430 | 850 | 1200 | 1500 | |
| | UVA | 370 | 450 | 1200 | 1600 | 2100 | |
| | UVA | 330 | 880 | 1700 | 2800 | 3200 | |
| | UVB | 289 | 1280 | 2100 | 2700 | 3200 | |
| | Dark | | 160 | 400 | 440 | 630 | |
| | Visible | 510 | 260 | 340 | 540 | 620 | |
| | Visible | 460 | 440 | 530 | 760 | 980 | |
| | Visible | 410 | 370 | 630 | 940 | 1200 | |
| | UVA | 390 | 490 | 940 | 1100 | 1500 | |
| | UVA | 370 | 660 | 1400 | 1700 | 2200 | |
| | UVA | 330 | 1300 | 2400 | 2700 | 3000 | |
| | UVB | 289 | 1800 | 3100 | 3800 | 4700 | |
| | Dark | | 210 | 390 | 610 | 820 | |
| | Visible | 510 | 180 | 380 | 560 | 800 | |
| | Visible | 460 | 320 | 590 | 820 | 1100 | |
| | Visible | 410 | 220 | 430 | 620 | 830 | |
| | UVA | 390 | 340 | 670 | 1000 | 1300 | |
| | UVA | 370 | 480 | 1000 | 1400 | 1800 | |
| | UVA | 330 | 750 | 1600 | 2200 | 2800 | |
| | UVB | 289 | 1300 | 2400 | 3300 | 4000 | |
| | Nordic 11.1 | Dark | | 640 | 1100 | 1600 | 1900 |
| | | Visible | 510 | 640 | 1300 | 1800 | 2200 |
| | | Visible | 460 | 1300 | 2500 | 3300 | 4100 |
| | | Visible | 410 | 880 | 1700 | 2400 | 3000 |
| UVA | | 390 | 1600 | 2900 | 4000 | 4800 | |
| UVA | | 370 | 1500 | 2800 | 3800 | 4700 | |
| UVA | | 330 | 3000 | 3800 | 5200 | 6400 | |
| UVB | | 289 | 3300 | 5500 | 7400 | 8900 | |
| Dark | | | 770 | 1400 | 2000 | 2500 | |
| Visible | | 510 | 1100 | 1900 | 2600 | 3200 | |
| Visible | | 460 | 2000 | 4000 | 5000 | 5600 | |
| Visible | | 410 | 1300 | 2300 | 3200 | 3800 | |
| UVA | | 390 | 1500 | 2500 | 3300 | 4200 | |
| UVA | | 370 | 1800 | 3100 | 4200 | 4100 | |
| UVA | | 330 | 3000 | 4600 | 6000 | 7000 | |
| UVB | | 289 | 2800 | 4600 | 6200 | 7500 | |

Table 6. Photoefficiency for all experiments.

| DOC type and concentration (mg/L) | Light source | Filter central wavelength (nm) | Photoefficiency | | | | |
|-----------------------------------|----------------|--------------------------------|-----------------|----------------|----------------|----------------|-----|
| | | | 2 hours (pg/W) | 4 hours (pg/W) | 6 hours (pg/W) | 8 hours (pg/W) | |
| Suwannee 6.34 | Visible | 510 | 1.6 | 1.5 | 1.3 | 0.0042 | |
| | Visible | 460 | 2.3 | 1.9 | 1.6 | 0.44 | |
| | Visible | 410 | 10 | 10 | 10 | 3.2 | |
| | UVA | 390 | 58 | 57 | 53 | 27 | |
| | UVA | 370 | 77 | 100 | 91 | 63 | |
| | UVA | 330 | 190 | 180 | 200 | 140 | |
| | UVB | 289 | 320 | 260 | 220 | 160 | |
| | Visible | 510 | 2.2 | 1.4 | 1.5 | -0.013 | |
| | Visible | 460 | 3.0 | 1.8 | 1.7 | 0.60 | |
| | Visible | 410 | 16 | 13 | 13 | 6.0 | |
| | UVA | 390 | 67 | 64 | 52 | 28 | |
| | UVA | 370 | 110 | 120 | 99 | 68 | |
| | UVA | 330 | 290 | 270 | 200 | 130 | |
| | UVB | 289 | 440 | 390 | 320 | 250 | |
| | Visible | 510 | 1.8 | 1.9 | 1.9 | -0.047 | |
| | Visible | 460 | 2.6 | 2.4 | 2.2 | 0.54 | |
| | Visible | 410 | 10 | 10 | 10 | 0.17 | |
| | UVA | 390 | 50 | 50 | 50 | 19 | |
| | UVA | 370 | 88 | 92 | 85 | 46 | |
| | UVA | 330 | 169 | 180 | 170 | 110 | |
| | UVB | 289 | 330 | 300 | 280 | 200 | |
| | Nordic 11.1 | Visible | 510 | 8.7 | 8.6 | 8.1 | 1.0 |
| | | Visible | 460 | 16 | 15 | 13 | 6.4 |
| | | Visible | 410 | 62 | 59 | 55 | 18 |
| | | UVA | 390 | 340 | 310 | 277 | 150 |
| | | UVA | 370 | 350 | 330 | 300 | 162 |
| | | UVA | 330 | 800 | 510 | 460 | 300 |
| | | UVB | 289 | 870 | 740 | 660 | 470 |
| Visible | | 510 | 1.3 | 0.99 | 0.86 | 0.79 | |
| Visible | | 460 | 5.5 | 5.6 | 4.5 | 3.5 | |
| Visible | | 410 | 5.6 | 4.6 | 4.0 | 3.3 | |
| UVA | | 390 | 160 | 120 | 97 | 92 | |
| UVA | | 370 | 250 | 200 | 180 | 160 | |
| UVA | | 330 | 600 | 430 | 360 | 310 | |
| UVB | | 289 | 540 | 430 | 380 | 340 | |

3.3 More DGM production data from different mercury and DOC concentration

Numerous round of experiment were conducted under different mercury and DOC condition, light intensity, and exposure time (Table 7). Two rounds of experiment were conducted by collecting DGM every 15 to 20 minutes, and beside the collecting time, DGM would just released to the environmental chamber. Overall, these data still showed

photoefficiency increased with decreasing wavelength. Another finding is that narrow band wavelength of light would have higher photoefficiency than wide band wavelength of light. UV lights without filters can produced the highest DGM but because UV without filter can transmit very high intensity energy, UV lights would have the lowest photoefficiency. We didn't take these data into the main chapter because at that time we didn't understand sometimes the background signal would be as high as dark and the gold traps we used sometimes had extremely high/low concentrations. The reader is cautioned that the recorded values might not be accurate for discussion. We later increased the mercury concentration in solution so the background signals won't affect the true DGM values and we also fabricated new sets of gold traps to collect more accurate data.

Table 7 DGM production under different DOC and mercury concentration.

| DOC type and concentration (mg/L) | Total Hg (ng/L) | Light source | Filter central wavelength (nm) | Cumulative DGM (pg) | Absorbed light (W) | DGM production rate (pg/L min) | Photo-efficiency (pg/W) | |
|-----------------------------------|-----------------|----------------------------------|--------------------------------|---------------------|--------------------|--------------------------------|-------------------------|-----|
| Suwannee 2.49 | 100 | Dark | | 170 | | 9.1 | | |
| | | Visible | 510 | 220 | 15 | 12 | 3.3 | |
| | | Visible | 460 | 210 | 23 | 11 | 1.8 | |
| | | Collecting DGM every 75 minutes. | Visible | 410 | 210 | 4.6 | 11 | 9.5 |
| | | Light exposure 525 mins | UVA | 370 | 260 | 11 | 14 | 8.1 |
| | | | UVB | 330 | 240 | 11 | 13 | 7.0 |
| Suwannee 2.49 | 100 | Dark | | 910 | | 140 | | |
| | | Fluorescence | 460 | 940 | 8.3 | 150 | 7.3 | |
| | | Fluorescence | 410 | 1100 | 1.7 | 170 | 140 | |
| | | Collecting DGM every 20 minutes. | UVA | 370 | 1100 | 4.1 | 160 | 34 |
| | | Light exposure 450 mins | UVB | 289 | 1200 | 0.68 | 190 | 490 |
| | | | UVA | none | 2600 | 990 | 390 | 1.6 |
| Suwannee 2.68 | 0.1 | Dark | | 910 | | 43 | | |
| | | UVA | 330 | 1000 | 7.9 | 47 | 11 | |
| | | UVB | 289 | 1100 | 9.8 | 53 | 20 | |
| | | Collecting DGM every 15 minutes. | UVA | none | 1300 | 260 | 63 | 2.0 |
| | | Light exposure 600 mins | UVB | none | 2100 | 200 | 99 | 7.0 |

3.4 Excitation Emission Matrices (EEMs) detail

We can obtain useful information by studying the peak values from the EEMs. The A, B, C, M peaks are discussed in the Chapter 2, and the HIX (humification index), BIX (biological index), M/C (carbon degraded level) etc. can also help us understand the DOC more (Table 8). From Table 8, we can also know that all the solution after light exposure didn't show large difference compared to each other.

Table 8. Excitation Emission Matrices (EEMs) peak values

| | Daily R.U.: | Max Fl | Ex | Max Fl | Em | Max Fl | B: | T: | A: | C: | M: | N: | McKnight: |
|--------------|-------------|--------|--------|---------|--------|--------|---|--------|--------|--------|--------|----|-----------|
| Suwannee NOM | 2.3475 | 250 | Max Fl | 15.2264 | 1.3500 | 1.7967 | 10.5375 | 8.5300 | 5.4393 | 3.3216 | 0.9733 | | |
| Before EXP | 2.3475 | 250 | 461 | 13.5770 | 1.2856 | 1.5359 | 9.3603 | 7.5120 | 4.6741 | 2.7048 | 0.9685 | | |
| dark | 2.3475 | 250 | 460 | 12.6608 | 0.9299 | 1.2136 | 8.8441 | 7.1704 | 4.4260 | 2.5003 | 0.9808 | | |
| 510 | 2.3475 | 250 | 461 | 13.3102 | 1.0092 | 1.4783 | 9.1993 | 7.4503 | 4.5868 | 2.5395 | 0.9536 | | |
| 460 | 2.3475 | 250 | 459 | 13.4044 | 0.9056 | 1.3400 | 9.2800 | 7.6239 | 4.6700 | 2.6689 | 0.9659 | | |
| 410 | 2.3475 | 250 | 459 | 14.3407 | 1.0475 | 1.5167 | 9.6925 | 7.9370 | 4.8018 | 2.8498 | 0.9897 | | |
| 390 | 2.3475 | 250 | 457 | 12.8108 | 0.9495 | 1.3737 | 8.9748 | 7.3275 | 4.5293 | 2.6927 | 0.9640 | | |
| 370 | 2.3475 | 250 | 465 | 13.3485 | 1.1129 | 1.5391 | 9.2485 | 7.4263 | 4.6148 | 2.7265 | 0.9553 | | |
| 330 | 2.3475 | 250 | 460 | 13.1181 | 0.8482 | 1.4326 | 9.1161 | 7.4437 | 4.5694 | 2.7074 | 0.9658 | | |
| 289 | 2.3475 | 250 | 465 | 13.2741 | 0.8391 | 1.3630 | 9.2285 | 7.5133 | 4.5743 | 2.5902 | 0.9460 | | |
| | HIX: | BIX: | T/B | T/M: | T/N: | T/C: | A/T: | A/C: | A/M: | M/C: | C/N: | | |
| Suwannee NOM | 8.3672 | 0.4415 | 1.3308 | 0.3303 | 0.5409 | 0.2106 | 5.8651 | 1.2353 | 1.9373 | 0.6377 | 2.5680 | | |
| Before EXP | 10.6622 | 0.4186 | 1.1947 | 0.3286 | 0.5678 | 0.2045 | 6.0944 | 1.2461 | 2.0026 | 0.6222 | 2.7772 | | |
| dark | 10.5545 | 0.4305 | 1.3051 | 0.2742 | 0.4854 | 0.1693 | 7.2873 | 1.2334 | 1.9982 | 0.6173 | 2.8678 | | |
| 510 | 11.3602 | 0.4131 | 1.4649 | 0.3223 | 0.5821 | 0.1984 | 6.2228 | 1.2348 | 2.0056 | 0.6157 | 2.9338 | | |
| 460 | 11.1360 | 0.4273 | 1.4797 | 0.2869 | 0.5021 | 0.1758 | 6.9252 | 1.2172 | 1.9872 | 0.6125 | 2.8566 | | |
| 410 | 10.8558 | 0.4371 | 1.4480 | 0.3159 | 0.5322 | 0.1911 | 6.3905 | 1.2212 | 2.0185 | 0.6050 | 2.7851 | | |
| 390 | 10.1333 | 0.4302 | 1.4468 | 0.3033 | 0.5102 | 0.1875 | 6.5331 | 1.2248 | 1.9815 | 0.6181 | 2.7213 | | |
| 370 | 10.7866 | 0.4147 | 1.3830 | 0.3335 | 0.5645 | 0.2072 | 6.0090 | 1.2454 | 2.0041 | 0.6214 | 2.7238 | | |
| 330 | 10.7533 | 0.4214 | 1.6890 | 0.3135 | 0.5291 | 0.1925 | 6.3634 | 1.2247 | 1.9950 | 0.6139 | 2.7494 | | |
| 289 | 10.7735 | 0.4168 | 1.6243 | 0.2980 | 0.5262 | 0.1814 | 6.7709 | 1.2283 | 2.0175 | 0.6088 | 2.9006 | | |
| | Daily R.U.: | Max Fl | Ex | Max Fl | Em | Max Fl | B: <td>T:</td> <td>A:</td> <td>C:</td> <td>M:</td> <td>N:</td> <td>McKnight:</td> | T: | A: | C: | M: | N: | McKnight: |
| Noridc NOM | 2.3110 | 245 | 427 | 10.2631 | 1.1074 | 1.2061 | 7.0431 | 5.5034 | 3.7597 | 2.2481 | 1.0106 | | |
| Before EXP | 2.3110 | 250 | 440 | 8.0636 | 1.4043 | 0.9120 | 5.5691 | 4.4221 | 2.8644 | 1.5959 | 1.0226 | | |
| dark | 2.3110 | 250 | 457 | 7.9002 | 0.5437 | 0.6491 | 5.5307 | 4.4072 | 2.7830 | 1.4667 | 1.0066 | | |
| 510 | 2.3110 | 250 | 466 | 8.5525 | 0.6031 | 0.6960 | 5.9812 | 4.8408 | 2.7997 | 1.6495 | 1.1303 | | |
| 460 | 2.3110 | 250 | 467 | 8.0350 | 0.4141 | 0.7828 | 5.8203 | 4.5602 | 2.8049 | 1.6523 | 1.0121 | | |
| 410 | 2.3110 | 250 | 462 | 8.1809 | 0.6376 | 0.6242 | 5.6172 | 4.4626 | 2.7739 | 1.4640 | 1.0245 | | |
| 390 | 2.3110 | 250 | 463 | 7.8683 | 0.5249 | 0.6905 | 5.4692 | 4.3627 | 2.7206 | 1.4570 | 0.9928 | | |
| 370 | 2.3110 | 250 | 440 | 7.7829 | 0.5676 | 0.5854 | 5.4186 | 4.2758 | 2.7149 | 1.3508 | 1.0081 | | |
| 330 | 2.3110 | 250 | 464 | 7.7664 | 0.5879 | 0.8095 | 5.5308 | 4.4494 | 2.7647 | 1.6193 | 1.0607 | | |
| 289 | 2.3110 | 250 | 466 | 9.4636 | 0.5266 | 0.8619 | 6.5749 | 5.2865 | 2.9987 | 1.9027 | 1.1165 | | |
| | HIX: | BIX: | T/B | T/M: | T/N: | T/C: | A/T: | A/C: | A/M: | M/C: | C/N: | | |
| Noridc NOM | 7.9565 | 0.4311 | 1.0891 | 0.3208 | 0.5365 | 0.2191 | 5.8398 | 1.2798 | 1.8733 | 0.6832 | 2.4481 | | |
| Before EXP | 9.6351 | 0.4166 | 0.6494 | 0.3184 | 0.5715 | 0.2062 | 6.1065 | 1.2594 | 1.9442 | 0.6477 | 2.7709 | | |
| dark | 13.8168 | 0.4117 | 1.1938 | 0.2332 | 0.4425 | 0.1473 | 8.5210 | 1.2549 | 1.9873 | 0.6315 | 3.0049 | | |
| 510 | 14.3226 | 0.5083 | 1.1540 | 0.2486 | 0.4220 | 0.1438 | 8.5937 | 1.2356 | 2.1364 | 0.5783 | 2.9348 | | |
| 460 | 10.9334 | 0.4496 | 1.8905 | 0.2791 | 0.4737 | 0.1717 | 7.1799 | 1.2325 | 2.0038 | 0.6151 | 2.7599 | | |
| 410 | 13.5464 | 0.4150 | 0.9789 | 0.2250 | 0.4263 | 0.1399 | 8.9995 | 1.2587 | 2.0250 | 0.6216 | 3.0481 | | |
| 390 | 12.9393 | 0.4186 | 1.3156 | 0.2538 | 0.4739 | 0.1583 | 7.9207 | 1.2536 | 2.0103 | 0.6236 | 2.9944 | | |
| 370 | 13.8184 | 0.4184 | 1.0314 | 0.2156 | 0.4334 | 0.1369 | 9.2560 | 1.2673 | 1.9959 | 0.6349 | 3.1653 | | |
| 330 | 10.2972 | 0.4517 | 1.3770 | 0.2928 | 0.4999 | 0.1819 | 6.8324 | 1.2430 | 2.0005 | 0.6214 | 2.7476 | | |
| 289 | 12.0302 | 0.5241 | 1.6366 | 0.2874 | 0.4530 | 0.1630 | 7.6282 | 1.2437 | 2.1925 | 0.5672 | 2.7784 | | |

3.5 Mercury predicting model calculation

Exponential, power, and linear fit curves for photoefficiency are shown in Table 9. The parameters entering the RTbasic model are as follows: 41°22' N, 75°05'W, July 19, 2005 18:00:00 GMT, Ozone layer 275 DU, Surface air pressure 1000 millibars, surface albedo at >325 nm 0.12, surface albedo at <325 nm 0.08. Total column SO₂, Column air temperature offset, and total cloud optical depth are set to be 0. The reconstructed solar irradiance (Figure 23) is then times with the photoefficiency curve at each wavelength from 200 nm to 800 nm to obtain DGM prediction value.

Table 9. Fit curves used for photoefficiency

| Trendline type | DOC source | Trendline equation | R ² | |
|----------------|--------------|----------------------|-----------------------|-------|
| Exponential | Suwannee | $y=2E+08e^{-0.043x}$ | 0.932 | |
| | Nordic (old) | $y=3E+06e^{-0.029x}$ | 0.928 | |
| | Nordic (new) | $y=7E+06e^{-0.032x}$ | 0.850 | |
| Power | Suwannee | $y=4E+43x^{-16.51}$ | 0.884 | |
| | Nordic (old) | $y=7E+29x^{-10.89}$ | 0.886 | |
| | Nordic (new) | $y=7E+32x^{-12.13}$ | 0.827 | |
| Linear | Suwannee | Visible | $y= -0.031x + 15.46$ | 0.869 |
| | | UV | $y= -1.792x + 722.4$ | 0.999 |
| | Nordic (old) | Visible | $y= -0.171x + 87.29$ | 0.955 |
| | | UV | $y= -2.889x + 1242$ | 0.992 |
| | Nordic (new) | Visible | $y= -0.0254x + 14.22$ | 0.713 |
| | | UV | $y= -2.889x + 1242$ | 0.992 |

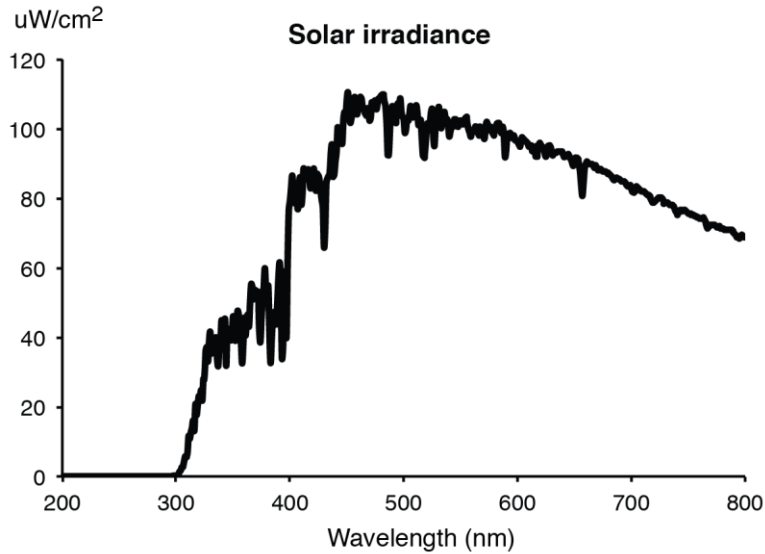


Figure 23. Reconstructed solar irradiance for Lake Gile at 1pm EST on July 19 2005.

3.6 Photoefficiency under different mercury concentration

Several rounds of experiments under different mercury concentration (with similar DOC concentration) were conducted, which might provide another way to examine the mercury concentration effect (Figure 24). We can observe that generally the photoefficiency seems to increase with increasing mercury concentration, but the trend is not very strong among the visible lights. Photoefficiency for UV lights below 390 nm demonstrates stronger positive correlation with mercury concentration.

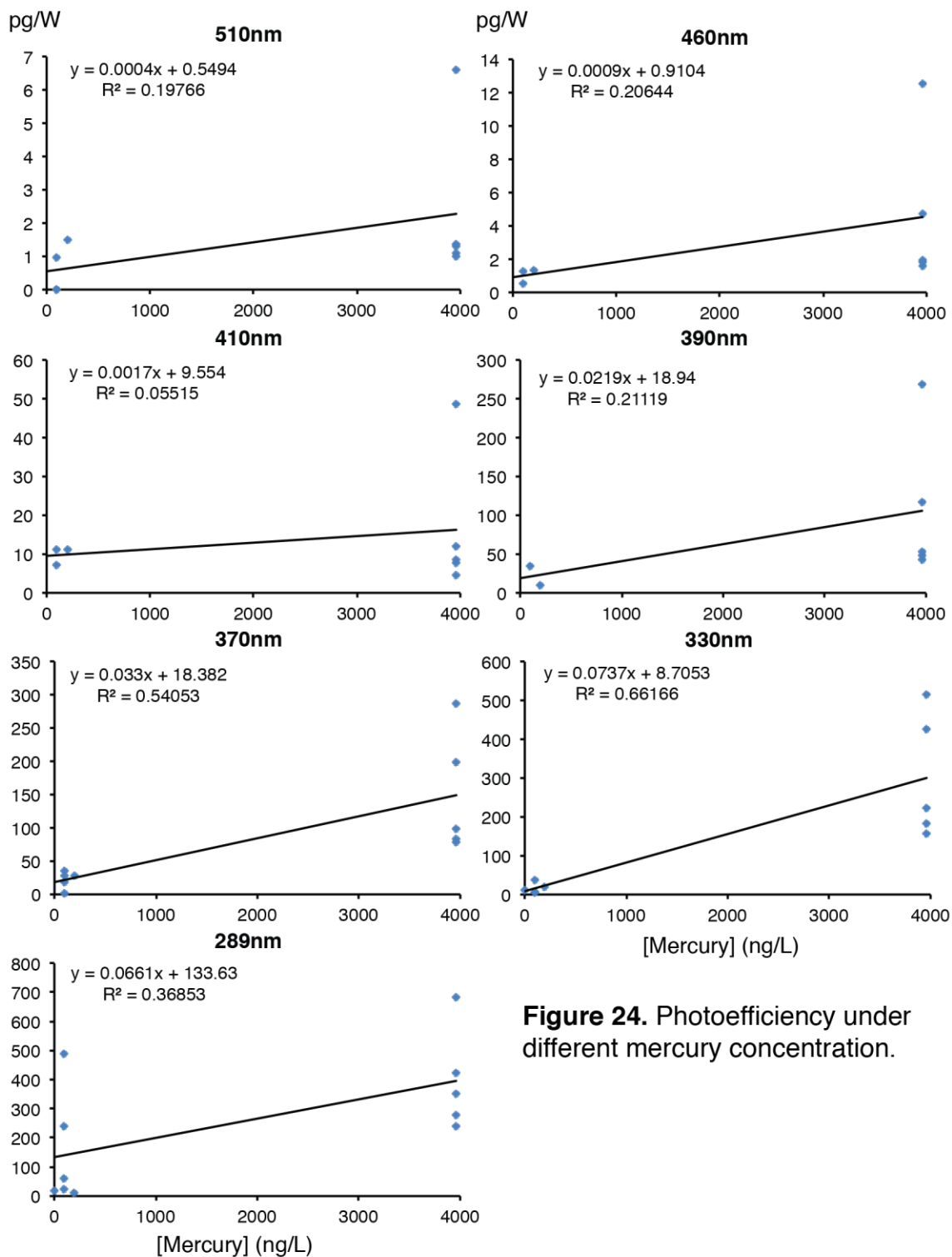


Figure 24. Photoefficiency under different mercury concentration.

3.7 Absorbance change over 105 hours under UVA and UVB exposure.

Suwannee River NOM solutions were exposed to UVA and UVB light with or without filter for 105 hours. Absorbance changes were measured (Figure 25-26) and show that the change increases as a function of exposure time and that UVB can cause more absorbance loss than UVA. Both UV light solutions with filters caused smaller absorbance changes than light without filters. From this testing experiment, we conclude that the DOC in solution won't undergo too much change if the solution is exposed to filtered light. Therefore, it's safe to discuss our result without considering changes of the solution's physical and chemical properties after 8 hours light exposure.

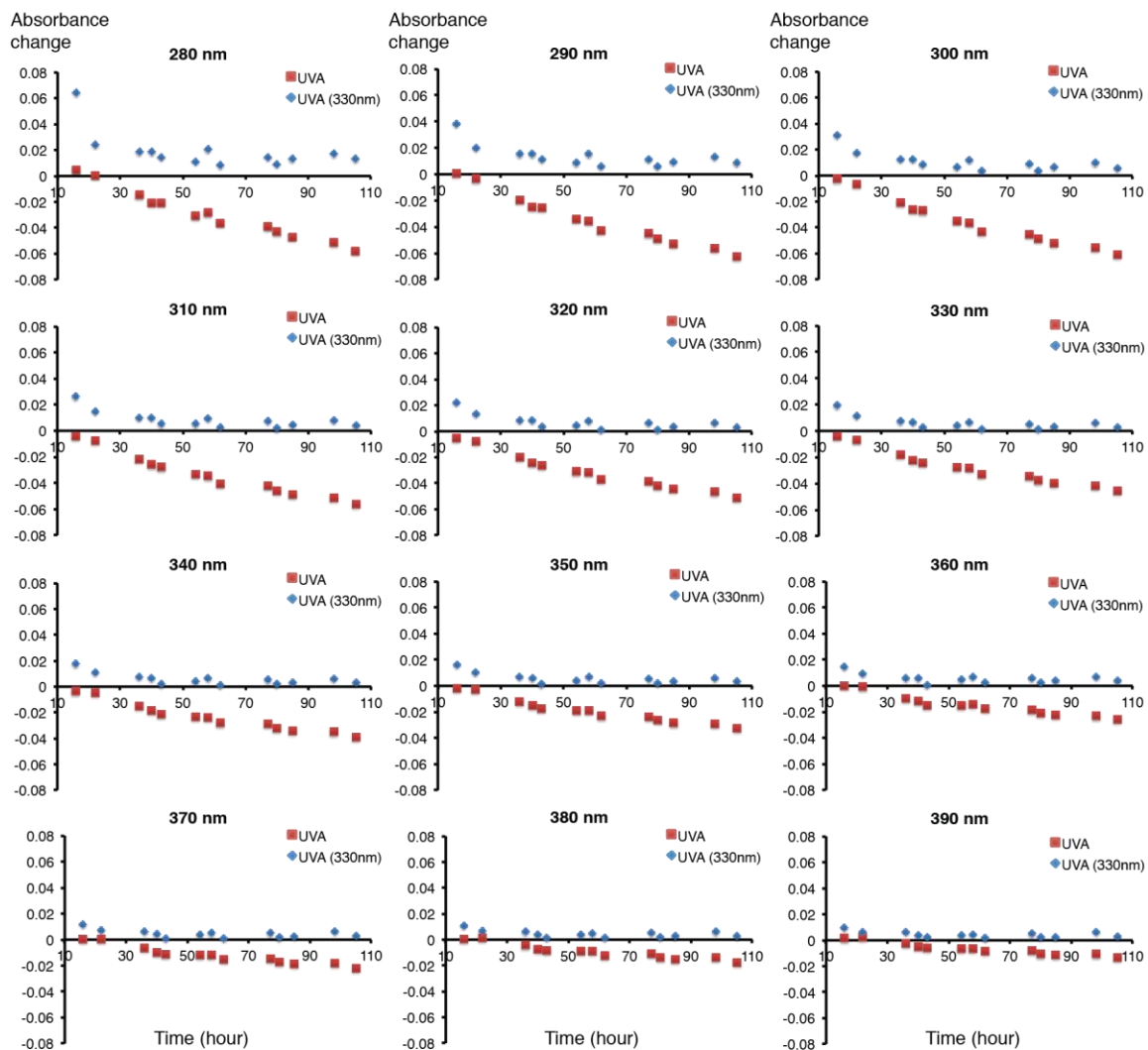


Figure 25. Absorbance change at specific wavelength for Suwannee River DOC solutions after 105 hours light exposure using UVA with/without filter.

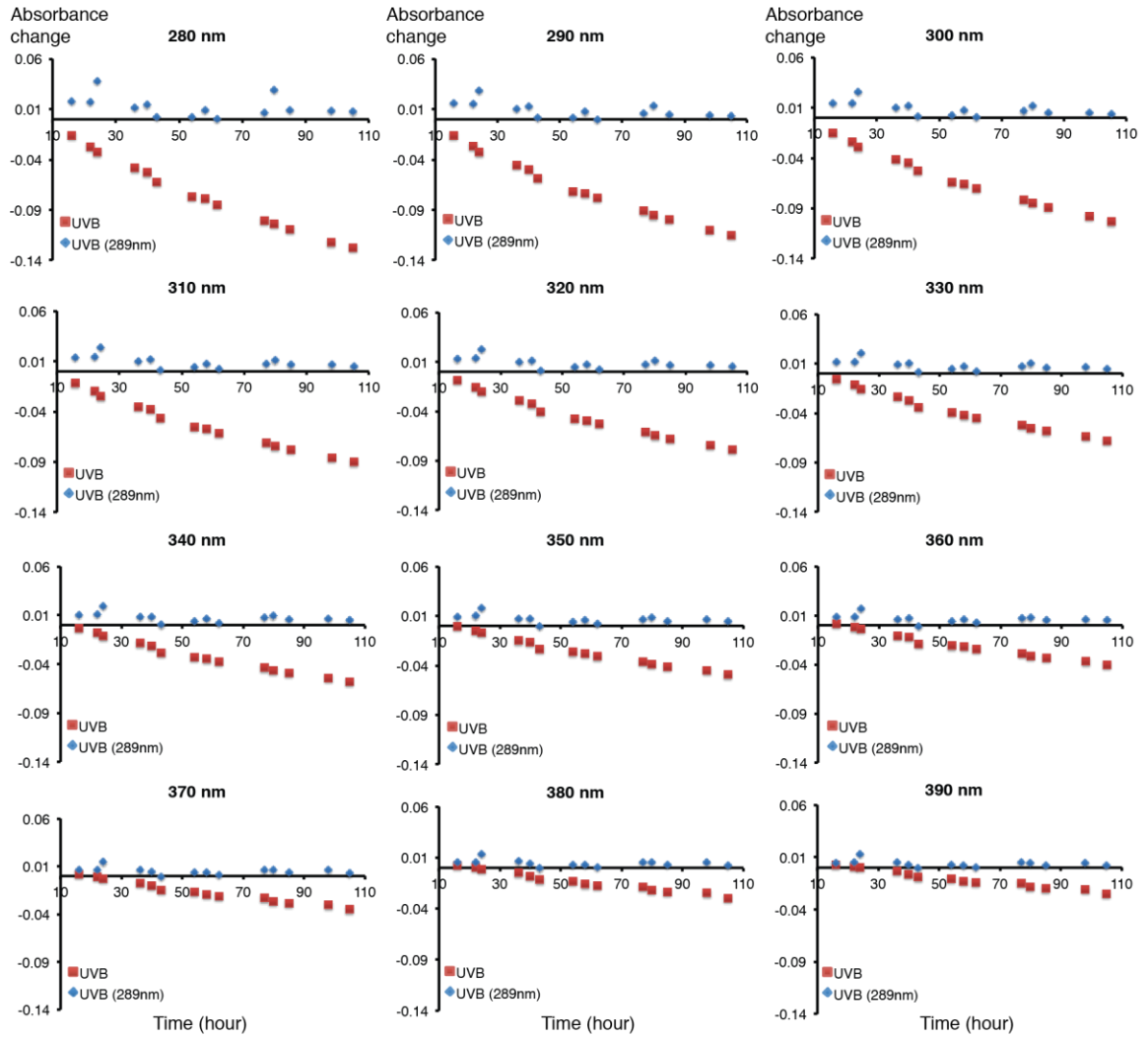


Figure 26. Absorbance change at specific wavelength for Suwannee River DOC solution after 105 hours light exposure using UVB with/without filter.

References

- Allard, B., Arsenie, I., 1991. Abiotic reduction of mercury by humic substances in aquatic system—an important process for the mercury cycle. *Water, Air, & Soil Pollution* 56, 457–464.
- Amyot, M., Lean, D., Mierle, G., 1997a. Photochemical Formation of volatile mercury in high Arctic lakes. *Environmental Toxicology and Chemistry* 16, 2054–2063.
- Amyot, M., McQueen, D.J., Mierle, G., Lean, D.R.S., 1994. Sunlight-Induced Formation of Dissolved Gaseous Mercury in Lake Waters. *Environ. Sci. Technol.* 28, 2366–2371.
- Amyot, M., Mierle, G., Lean, D., Mc Queen, D.J., 1997b. Effect of solar radiation on the formation of dissolved gaseous mercury in temperate lakes. *Geochimica et Cosmochimica Acta* 61, 975–987.
- Chai, X., Liu, G., Zhao, X., Hao, Y., Zhao, Y., 2012. Complexion between mercury and humic substances from different landfill stabilization processes and its implication for the environment. *Journal of Hazardous Materials* 209–210, 59–66.
- Clarkson, T.W., 2002. The three modern faces of mercury. *Environ Health Perspect* 110, 11–23.
- Coble, P.G., 1996. Characterization of marine and terrestrial DOM in seawater using excitation-emission matrix spectroscopy. *Marine Chemistry* 51, 325–346.
- Coble, P.G., Green, S.A., Blough, N.V., Gagosian, R.B., 1990. Characterization of dissolved organic matter in the Black Sea by fluorescence spectroscopy. *Nature* 348, 432–435.

- Fellman, J.B., Hood, E., Spencer, R.G.M., 2010. Fluorescence spectroscopy opens new windows into dissolved organic matter dynamics in freshwater ecosystems: A review. *Limnology and oceanography* 55, 2452–2462.
- Garcia, E., Amyot, M., Ariya, P., 2005. Relationship between DOC photochemistry and mercury redox transformations in temperate lakes and wetlands. *Geochimica et Cosmochimica Acta* 69, 1917–1924.
- Garcia, E., Poulain, A.J., Amyot, M., Ariya, P.A., 2005. Diel variations in photoinduced oxidation of Hg⁰ in freshwater. *Chemosphere* 59, 977–981.
- Haitzer, M., Aiken, G.R., Ryan, J.N., 2002. Binding of Mercury(II) to Dissolved Organic Matter: The Role of the Mercury-to-DOM Concentration Ratio. *Environ. Sci. Technol.* 36, 3564–3570.
- Her, N., Amy, G., McKnight, D., Sohn, J., Yoon, Y., 2003. Characterization of DOM as a function of MW by fluorescence EEM and HPLC-SEC using UVA, DOC, and fluorescence detection. *Water Research* 37, 4295–4303.
- Hesterberg, D., Chou, J.W., Hutchison, K.J., Sayers, D.E., 2001. Bonding of Hg(II) to Reduced Organic Sulfur in Humic Acid As Affected by S/Hg Ratio. *Environ. Sci. Technol.* 35, 2741–2745.
- Ishii, S.K.L., Boyer, T.H., 2012. Behavior of Reoccurring PARAFAC Components in Fluorescent Dissolved Organic Matter in Natural and Engineered Systems: A Critical Review. *Environ. Sci. Technol.* 46, 2006–2017.
- Kirk, J.T.O., 1994. *Light and Photosynthesis in Aquatic Ecosystems*, 2nd ed. Cambridge University Press.

- Krabbenhoft, D.P., Hurley, J.P., Olson, M.L., Cleckner, L.B., 1998. Diel variability of mercury phase and species distributions in the Florida Everglades. *Biogeochemistry* 40, 311–325.
- Lalonde, J.D., Amyot, M., Orvoine, J., Morel, F.M.M., Auclair, J.-C., Ariya, P.A., 2003. Photoinduced Oxidation of Hg⁰(aq) in the Waters from the St. Lawrence Estuary. *Environ. Sci. Technol.* 38, 508–514.
- Lochmueller, C.H., Saavedra, S.S., 1986. Conformational changes in a soil fulvic acid measured by time-dependent fluorescence depolarization. *Anal. Chem.* 58, 1978–1981.
- Mercury Study Report to Congress | Mercury | US EPA , 2012. URL <http://epa.gov/hg/report.htm>
- Mobed, J.J., Hemmingsen, S.L., Autry, J.L., McGown, L.B., 1996. Fluorescence Characterization of IHSS Humic Substances: Total Luminescence Spectra with Absorbance Correction. *Environ. Sci. Technol.* 30, 3061–3065.
- O’Driscoll, N.J., Beauchamp, S., Siciliano, S.D., Rencz, A.N., Lean, D.R.S., 2003. Continuous Analysis of Dissolved Gaseous Mercury (DGM) and Mercury Flux in Two Freshwater Lakes in Kejimikujik Park, Nova Scotia: Evaluating Mercury Flux Models with Quantitative Data. *Environ. Sci. Technol.* 37, 2226–2235.
- O’Driscoll, N.J., Lean, D.R.S., Loseto, L.L., Carignan, R., Siciliano, S.D., 2004. Effect of Dissolved Organic Carbon on the Photoproduction of Dissolved Gaseous Mercury in Lakes: Potential Impacts of Forestry. *Environ. Sci. Technol.* 38, 2664–2672.

- O'Driscoll, N.J., Siciliano, S.D., Lean, D.R.S., Amyot, M., 2005. Gross Photoreduction Kinetics of Mercury in Temperate Freshwater Lakes and Rivers: Application to a General Model of DGM Dynamics. *Environ. Sci. Technol.* 40, 837–843.
- Oh, S., Kim, M.-K., Lee, Y.-M., Zoh, K.-D., 2011. Effect of Abiotic and Biotic Factors on the Photo-Induced Production of Dissolved Gaseous Mercury. *Water, Air, & Soil Pollution* 220, 353–363.
- Osburn, C.L., Stedmon, C.A., 2011. Linking the chemical and optical properties of dissolved organic matter in the Baltic-North Sea transition zone to differentiate three allochthonous inputs. *Marine Chemistry*.
- Peters, S.C., Wollenberg, J.L., Morris, D.P., Porter, J.A., 2007. Mercury Emission to the Atmosphere from Experimental Manipulation of DOC and UVR in Mesoscale Field Chambers in a Freshwater Lake. *Environ. Sci. Technol.* 41, 7356–7362.
- Qureshi, A., O'Driscoll, N.J., MacLeod, M., Neuhold, Y.-M., Hungerbühler, K., 2009. Photoreactions of Mercury in Surface Ocean Water: Gross Reaction Kinetics and Possible Pathways. *Environ. Sci. Technol.* 44, 644–649.
- Ravichandran, M., 2004. Interactions between mercury and dissolved organic matter—a review. *Chemosphere* 55, 319–331.
- Skyllberg, U., Bloom, P.R., Qian, J., Lin, C.-M., Bleam, W.F., 2006. Complexation of Mercury(II) in Soil Organic Matter: EXAFS Evidence for Linear Two-Coordination with Reduced Sulfur Groups. *Environ. Sci. Technol.* 40, 4174–4180.
- Stedmon, C.A., Markager, S., Bro, R., 2003. Tracing dissolved organic matter in aquatic environments using a new approach to fluorescence spectroscopy. *Marine Chemistry* 82, 239–254.

- Stevenson, F.J., 1994. Humus chemistry: genesis, composition, reactions. John Wiley and Sons.
- Del Vecchio, R., Blough, N.V., 2004. On the Origin of the Optical Properties of Humic Substances. *Environ. Sci. Technol.* 38, 3885–3891.
- Vost, E.E., Amyot, M., O’Driscoll, N.J., n.d. Photoreactions of Mercury in Aquatic Systems, in: Liu, G., Cai, Y., O’Driscoll, N. (Eds.), *Environmental Chemistry and Toxicology of Mercury*. John Wiley & Sons, Inc., pp. 193–218.
- Whalin, L.M., Mason, R.P., 2006. A new method for the investigation of mercury redox chemistry in natural waters utilizing deflatable Teflon® bags and additions of isotopically labeled mercury. *Analytica Chimica Acta* 558, 211–221.
- Wollenberg, J.L., Peters, S.C., 2009. Diminished mercury emission from waters with duckweed cover. *J. Geophys. Res.* 114, 10 PP.
- Xia, K., Skyllberg, U.L., Bleam, W.F., Bloom, P.R., Nater, E.A., Helmke, P.A., 1998. X-ray Absorption Spectroscopic Evidence for the Complexation of Hg(II) by Reduced Sulfur in Soil Humic Substances. *Environ. Sci. Technol.* 33, 257–261.

Pin-Chin Hsu

213 East Morton St., Bethlehem, PA 18015

(626)-623-0887 pch210@lehigh.edu

Education

Lehigh University, Bethlehem, PA

Master of Science in Earth and Environmental Sciences May 2012

Thesis: Factors Influencing Mercury Photoreactions in Fresh Waters:
An Experimental Approach Using Light and DOC

Advisor: Prof. Stephen C. Peters

Ohio State University, Columbus, OH

Teacher Training Program for Chinese pedagogy, Summer Programs

East Asian Concentration August 2010

National Taiwan University, Taipei, Taiwan

Bachelor of Science, Chemistry June 2008

Research experience

Factors Influencing Mercury Photoreactions in Fresh Waters: An Experimental Approach Using Light and DOC– Master thesis topic from Lehigh University August 2010- May 2012

Analyzing and investigating the concentrations of arsenic and metal ions of ground water– Research assistant at National Taiwan University May 2009 - May 2010

Teaching experience

Lehigh University, Department of Modern Languages and Literature

Adjunct Lecturer

| | |
|---|-----------------------------|
| Intensive Chinese Conversation | January 2011 – May 2012 |
| Advanced Chinese Reading and Writing II | January 2012 – May 2012 |
| Intermediate Chinese Reading and Writing II | January 2012 – May 2012 |
| Advanced Chinese Reading and Writing I | August 2011 – December 2011 |
| Intermediate Chinese Reading and Writing I | August 2011 – December 2011 |
| Newspaper Reading in Chinese | January 2011 – May 2011 |
| Chinese Short Stories | January 2011 – May 2011 |
| Business Chinese | August 2010 – December 2010 |

Teaching Assistant

| | |
|--|-----------------------------|
| Advanced Spoken Chinese II (Prof. Shan) | January 2011 – May 2011 |
| Intermediate Spoken Chinese II (Prof. Shan) | January 2011 – May 2011 |
| Advanced Spoken Chinese I (Prof. Shan) | August 2010 – December 2010 |
| Intermediate Spoken Chinese I (Prof. Shan) | August 2010 – December 2010 |
| Beginning Spoken Chinese I (Prof. Shan) | August 2010 – December 2010 |
| Beginning Chinese Reading and Writing I (Prof. Yu) | August 2010 – December 2010 |

Honors

| | |
|--|---------------|
| Grants-in-Aid of Research- Sigma Xi, The Scientific research Society | December 2011 |
| Graduate Scholarship- Earth and Environmental Sciences, Lehigh University | May 2011 |
| Graduate Instructional Committee Research Funds- Lehigh University | April 2011 |
| Summer Programs East Asian Concentration Scholarship- | |

Ohio State University

May 2010

Outstanding Honorable Award- Ministry of Defense, Taiwan

February 2009

Commencement Representative- Department of Chemistry,

National Taiwan University

June 2008

Publication

Hsu, P.C., Peters, S.C. Hargreaves, B.R., Morris, D.P., 2011, Factors Influencing Mercury Photoreactions in Fresh Waters: An Experimental Approach Manipulating Light and DOC, Fall Meeting. B33H-0573.